

~~CONFIDENTIAL~~Copy 6
RM E52J23

JAN 9 1953

NACA

RESEARCH MEMORANDUM

PRELIMINARY EXPERIMENTS WITH PILOT BURNERS

FOR RAM-JET COMBUSTORS

By John M. Farley, Robert E. Smith, and John H. Povolny

Lewis Flight Propulsion Laboratory
Cleveland, Ohio

CLASSIFICATION CHANGED

UNCLASSIFIED

To _____

By authority of *NACA Records* *effective*
TRN-123 Date *Dec. 13, 1957**AMT 1-20-58*

CLASSIFIED DOCUMENT

This material contains information affecting the National Defense of the United States within the meaning of the espionage laws, Title 18, U.S.C., Secs. 793 and 794, the transmission or revelation of which in any manner to an unauthorized person is prohibited by law.

NATIONAL ADVISORY COMMITTEE
FOR AERONAUTICS

WASHINGTON

January 2, 1953

NACA LIBRARY
LANGLEY AERONAUTICAL LABORATORY
Langley Field, Va.~~CONFIDENTIAL~~

NACA RM E52J23

NATIONAL ADVISORY COMMITTEE FOR AERONAUTICS

RESEARCH MEMORANDUM

PRELIMINARY EXPERIMENTS WITH PILOT BURNERS FOR RAM-JET COMBUSTORS

By John M. Farley, Robert E. Smith*, and John H. Povolny

SUMMARY

As part of an over-all program to develop a high-altitude, low-drag ram-jet combustor, a preliminary development program on can-type pilot burners has been conducted at the Lewis laboratory. A 5-inch-diameter circular pilot burner and an annular-segment pilot burner were developed which gave stable operation over a satisfactory range of fuel-air ratios with static-pressure ratios across the pilot burner from about 1.02 to 1.08 with an inlet pressure of 10 inches of mercury absolute. With fuel injected about 12 inches upstream of the annular-segment pilot burner, a combustion efficiency of 61 percent was obtained at a fuel-air ratio of 0.06, with an inlet pressure of 10 inches of mercury absolute. Efficiencies over 80 percent were obtained with a homogeneous fuel-air mixture, and it is believed that with some detailed fuel-system studies such values are attainable when the fuel is injected within 12 inches of the pilot-burner dome.

INTRODUCTION

Recent investigations of ram-jet engines have indicated that the stability on low-drag ram-jet combustors operating at combustor-inlet pressures in the order of $1/2$ atmosphere and less may be improved by use of a stable heat source or pilot flame (reference 1). In the past, pilot-burner air flows have generally been about 1 or 2 percent of the total air flow. However, by use of low-drag pilot configurations, pilot air flows as high as 8 percent of the total, with a blocked area of about 25 percent of the ram-jet combustor cross-sectional area, appear feasible. Combustors using can-type burners of relatively low drag have shown good stability and efficiency characteristics with inlet pressures as low as 8 inches of mercury absolute and therefore appear well suited to pilot applications (references 2 and 3). As part of an over-all program to develop a high-altitude, low-drag ram-jet combustor, an experimental investigation of some of the pertinent design features of can-type pilot burners has been conducted at the NACA Lewis laboratory.

*Mr. Smith, of ARO Inc., is on assignment to the NACA Lewis laboratory.

Annular-segment configurations and circular can-type pilot burners (5-in. diam.) with a single row and also with six rows of holes were investigated at inlet pressures from 10 to 30 inches of mercury absolute, with static-pressure ratios across the pilot burners ranging from about 1.02 to 1.10. To eliminate the effect of fuel distribution, a long mixing length was used for most of the investigations (about 11 ft for circular pilot burners and about 9 ft for annular-segment burners), so that the fuel-air mixture was essentially homogeneous. A brief investigation of more realistic fuel systems was also included in the program. Inlet-air temperatures ranged from about 100° to 300° F.

PRELIMINARY CONSIDERATIONS

In an investigation of can-type pilot burners with one and two rows of holes, Longwell (reference 3) found that the best operation was obtained when the sum of the diameters of the holes in the first row was about 40 percent of the can perimeter at the first row. Longwell also determined that the stability of a two-row pilot burner could be fairly well correlated in terms of the air flow through the first row of holes. The effect of varying first-row total hole area by using various size holes was, however, not determined. In view of the apparent importance of the first row, it was decided first to investigate single-row configurations in order to determine the optimum hole size while maintaining the percentage of open perimeter at 40 percent. The performance of multi-row configurations was determined with the first-row holes at optimum size on the basis of results of the first investigation.

Analysis of flow conditions in a ram-jet combustor using a low-drag can-type pilot burner (appendix A) indicates that the percentage of total air flow that may be expected to pass through the pilot burner is approximately 0.35 of the percentage of cross-sectional area blocked by the pilot burner. In order to obtain a pilot air flow of 8 percent of the total air flow, a circular pilot diameter of nearly 1/2 the ram-jet-combustor diameter would be required. In a large-diameter ram-jet combustor such a pilot burner would be excessively long and bulky. However, by using an annular cross section, a pilot burner could be built which would pass the required amount of air and still be of such scale that a segment of the pilot burner could be developed in the available facility. Therefore, it was decided that the development of a satisfactory annular-segment pilot burner would also be desirable at this time. Annular pilots have the additional advantage of providing better distribution of the stabilizing flame throughout the cross section of the ram-jet combustor and when placed in the combustor-inlet diffuser can be designed to divide the diffuser into coaxial channels and allow more efficient diffusion.

APPARATUS

2687 A sketch of the apparatus used for the investigation of the 5-inch-diameter pilot burners is shown in figure 1. A photograph of the test section and transition sections used in the investigation of the annular-segment pilots is presented in figure 2. In both investigations the air flow was set by choking a valve in the inlet-air line. Air flows were measured with a variable-area orifice in the combustion-air line. Exhaust pressures were set with either the exhaust-pressure regulating valve, or with the flapper valve shown in figure 1. For the annular-segment investigations the flapper valve was replaced with a butterfly valve located at the outlet of the exhaust transition section. Water-spray bars for quenching the combustion gases were located just downstream of the flapper valve in the circular setup and about 1 inch downstream of the pilot outlet in the annular-segment setup. A temperature survey for the spray-cooled exhaust products was located just upstream of the exhaust-pressure regulating valve.

A photograph of a typical multirow circular pilot burner is presented in figure 3. Table I gives the characteristics of the various circular configurations investigated. Three single-row configurations having hole diameters of $1/4$, $1/2$, and $3/4$ inch were investigated (configuration A). Multirow configurations B and C had identical first rows (nine $1/2$ -in.-diam. holes). In configuration B the hole-area distribution in the last five rows was axially parabolic to give more gradual addition of mixture to the burner in the early rows; whereas, in configuration C there was an equal amount of hole area in each of the last five rows, that is, linear hole distribution. Configuration D had six $3/4$ -inch-diameter holes in the first row and parabolic distribution in the last five rows. The various modifications of the annular-segment pilot burner are given in table II. The basic annular-segment pilot-burner configuration investigated (AA) had parabolic hole distribution in the last five rows. A photograph of a modification of this configuration is presented in figure 4.

A sketch of an air-atomizing fuel spray bar typical of those used for injection at the upstream station (station 1 in fig. 1) for both the circular and annular-segment pilot burners is presented in figure 5(a). Modifications of this fuel bar, having different numbers of orifices, were used for various fuel-flow ranges. Fuel bars used for injection 6 to 12 inches upstream of the burner in the annular-segment pilot-burner investigation are shown in figures 5(b) and 5(c). A photograph of several of the fuel bars used is presented in figure 6.

An externally mounted oxygen-hydrogen igniter was used. The igniter flame passed through one of the hollow mounting struts into the dome of the pilot burner. A water-cooled plexiglass window was provided in the outer surface of each test section to allow visual observation of pilot-burner operation.

Unleaded gasoline (MIL-F-5572, grade 80) with a lower heating value of 18,850 Btu per pound was used throughout the investigation.

Instrumentation. - A sketch showing test-section instrumentation is included in figure 1. The pilot-burner-inlet total and static pressures were measured at station 2. Changes in the static pressure of the air flowing in the annulus between the burner and test-section wall were measured with a line of wall static taps. At station 3 there were three wall static taps to measure pilot-outlet static pressure. Fuel flows and spray-water flows were measured with calibrated rotameters. Cooling-jacket water flows were determined from the cooling-water-manifold pressure and a calibration curve of flow against pressure. Inlet and outlet temperatures of the jacket cooling water were recorded. Pressures were measured with manometers and temperatures were measured with thermocouples.

Procedure. - The investigations were conducted over a range of inlet static pressures from about 10 to 30 inches of mercury absolute, and with a range of static-pressure ratios across the pilot burners from 1.02 to about 1.10. The procedure used was to set an air flow which gave approximately the desired pressure ratio at a given value of inlet pressure and then to record data over the full range of operable fuel-air ratios while maintaining air flow and inlet pressure constant. The pilot burners were also investigated under cold-flow conditions in order to determine the cold drag coefficients.

Most of the investigations were conducted with air-atomizing fuel spray bars (fig. 5(a)) placed well upstream of the pilots (station 1, fig. 1) to obtain homogeneous fuel-air mixtures. A brief investigation was also conducted to determine the effect of various fuel distributions and injection positions with both the circular- and annular-segment-type pilot burners. (Hereinafter, upstream fuel injection will be referred to as homogeneous fuel injection.) Combustion efficiencies were determined from a heat balance between the pilot-burner inlet and the cooled exhaust-gas-temperature survey stations (stations 2 and 4, respectively, fig. 1). Both spray-water and exhaust-pipe cooling-jacket-water flows were accounted for in the heat balance. Combustion efficiencies were then calculated from the following equation:

$$\eta_b = \frac{W_e(H_{s,4} - H_{w,1}) + W_a(H_{g,4} - H_{g,2}) + W_j(H_{w,o} - H_{w,i})}{(18,850)W_f}$$

(Symbols are defined in appendix B.) With the single-row circular pilot burners, the air flows were much lower than the values for which the test rig was originally designed; therefore, it was not possible to obtain combustion efficiencies. With the multirow circular pilot burners the efficiency values obtained were, in general, somewhat doubtful

for the same reason. Therefore, only stability data are presented for these configurations. Inlet Mach numbers to the pilot burner were calculated with measured values of air flow, pilot-inlet static pressure, pilot-inlet temperature, and pilot cross-sectional area.

DISCUSSION OF RESULTS

Single-Row Circular Pilot Burners

Typical results showing blow-out limits of the single-row pilot burners are presented in figure 7. For the configurations shown, the number and the diameter of the holes were varied, but the ratio of the sum of the hole diameters to the perimeter of the burner was held constant (approximately 40 percent).

These results indicate that within the accuracy of the data the hole size had no significant effect on the lean blow-out limits over the range of pressure ratios investigated (1.015 to 1.113). The lean blow-out limits for each of the configurations varied from 0.023 to 0.044. On the other hand, hole diameter had a pronounced effect on the rich blow-out limits. The blow-out fuel-air ratios were highest for the configuration having nine 1/2-inch-diameter holes, varying from 0.146 at a pressure ratio of 1.023 to 0.093 at a pressure ratio of 1.113. The rich fuel-air ratio blow-out limits were about 0.02 and 0.04 lower for the configurations having 3/4-inch- and 1/4-inch-diameter holes, respectively. During operation it was observed that with the 1/2-inch-diameter and 3/4-inch-diameter hole configurations, the fuel-air mixture burned with a blue flame over the entire cross section. With the 1/4-inch-diameter hole configuration, the mixture burned with a blue core surrounded by an orange flame. The different burning phenomena may have resulted from variation in penetration and subsequent mixing within the combustion zone.

The data presented in figure 7 indicate the combustion limits but do not differentiate between stable and unstable combustion. During operation of the pilot burners it was found that the practical operating range of each single-row configuration was restricted to a considerably narrower range of fuel-air ratios than that indicated by the blow-out limits because of unstable combustion characteristics in the fringe areas of rich and lean blow-out. In terms of stable operating range, the 1/2-inch-diameter hole configuration was still the best single-row configuration investigated. The instability regions for this configuration are shown in figure 8. The width of the rich unstable region was different for each configuration and varied with inlet pressure but was not affected appreciably by variations in pressure ratio for the given configuration and inlet pressure. In each case, as the rich blow-out limit was approached, the flame began to flash intermittently from the

outlet end of the pilot back through the outer annulus and upstream of the pilot dome. The frequency and severity usually increased as rich blow-out limit was more nearly approached. As the lean blow-out limit was approached there was a tendency for the flame in the dome to blow out so that burning existed only downstream of the holes. The range of fuel-air ratios in which unstable combustion occurred was, in general, narrower near lean blow-out than in the region of rich blow-out.

The range of operation of each of the single-row configurations increased when the inlet pressure was decreased. This effect of inlet pressure on the blow-out limits of the 1/2-inch-hole configuration is shown in figure 9. With a pressure ratio of 1.06 the operable fuel-air-ratio range was from about 0.04 to 0.103 with an inlet pressure of 30 inches of mercury absolute, and from about 0.025 to 0.145 with an inlet pressure of 10 inches of mercury absolute. This reversal of the usual effect of pressure on combustion was caused by the increased tendency of the pilot burners to flash back and become unstable at higher values of inlet pressure. Because the object of the single-row investigation was to find the optimum size for the first-row holes, it was decided that a study to eliminate flashback would be reserved for the investigation of the configuration with more than one row of holes.

Several methods of injecting fuel at distances varying from 8 to 15 inches upstream of the pilot-burner dome were tried. All these fuel-system variations proved unsatisfactory, however, because of improper fuel vaporization and liquid fuel impinging on and running down the walls of the inlet pipe. This led to burning outside the pilot burner and to unstable operation.

Six-Row Circular Pilot Burners

Two six-row pilot-burner configurations were fabricated, each having nine 1/2-inch-diameter holes in the first row, in accordance with the results of the preliminary single-row investigation. The hole-area distribution in the last five rows of one configuration was parabolic axially, and in the other configuration the distribution was linear (configurations B and C).

Effect of annular opening at pilot-burner outlet. - The parabolic hole-distribution configuration was first investigated with an annular opening between the pilot burner and the outer pipe in the plane of the pilot-burner outlet (configuration B1). As for the configuration with a single row of holes, considerable flashback through the annulus occurred, particularly at low values of pressure ratio and at the higher values of inlet pressure. The flashback tendencies increased when the exhaust pressure was regulated by means of the flapper valve just aft of the pilot burner, a condition which was later found to be true for most

other configurations investigated. Therefore, in this and in subsequent investigations exhaust pressure was regulated with the valve located farther downstream in the exhaust system. In an effort to broaden the stability limits, the annular opening was closed by flaring out the aft end of the pilot burner (configuration B2). A comparison of the stable operating ranges of configurations B1 and B2 is made in figure 10. Closing the annulus resulted in an extension of the operable fuel-air-ratio range at the lower values of pressure ratio at each of the inlet pressures investigated. With a pressure ratio of 1.03 and an inlet pressure of 10 inches of mercury absolute, the operable range of fuel-air ratios was from 0.053 to 0.094 with the annulus open and from 0.053 to 0.123 with the annulus closed. With this inlet pressure, the maximum operable pressure ratio was increased from about 1.07 with the annulus open to about 1.08 with it closed. Although the configuration with the closed annulus operated more smoothly than the open-annulus configuration, some burning upstream of the pilot burner still occurred at values of pressure ratio below 1.04. With inlet pressures of 10 and 20 inches of mercury absolute, this upstream burning was in form of a halo and had no apparent detrimental effect on the pilot performance. At 30 inches of mercury absolute, the upstream burning caused some overheating of the pilot burner.

Effect of hole-area distribution. - The linear hole-area configuration was also investigated with the annulus at the exit of the pilot burner open and with the annulus closed (configurations C1 and C2). Results of these tests were essentially the same as those for the corresponding parabolic hole configurations (B1 and B2); that is, the change in hole-area distribution had negligible effect on performance.

Effect of first-row hole modification. - The limits shown in figure 10 are stable operation limits and do not necessarily indicate blow-out of the complete pilot burner. With most conditions of inlet pressure and pressure ratio, the lean stability limit was characterized by blow-out of the pilot burner downstream of the first row of holes, combustion being maintained in the dome. The same phenomenon was noted at the rich stability limit with the higher values of pressure ratio and lower values of inlet pressure. When operating at fuel-air ratios very near the lean stability limit, it was sometimes possible to obtain a condition in which the downstream portion of the pilot burner would blow out and relight in regular cycles with a frequency on the order of 2 cycles per second. When downstream blow-out occurred, dark jets of incoming mixture could be seen at the second row of holes penetrating into the flame coming from upstream in the dome, which indicated that the mixture flow through the second row was quenching the first-row flame.

In an effort to reduce quenching and to extend the operating range, two modifications were tried. The first modification was an attempt to increase penetration of the first-stage mixture by adding internal scoops

or "thimbles" to the downstream side of the first row of holes and on four of the second-row holes (configuration C3). These thimbles are illustrated in figure 11. This modification resulted in an increased tendency to flashback and reduced stability limits. There was a tendency for balls of flame to seat on the upstream face of the thimbles and propagate from there to the outside of the burner.

The second modification was an attempt to increase the proportion of mixture to the first row by using six 3/4-inch-diameter holes in place of the 1/2-inch-diameter holes (configuration D). This modification had no significant effect on the performance.

Effect of annular passage size. - In order to determine the effect of the size of the annular passage between the pilot burner and the outer pipe, two venturi-shaped tubes or shrouds were fabricated which could be placed around the burner to reduce the annular area (see table I). Without a shroud the burner blocked about 50 percent of the pipe area in the plane of the center line of the first-row holes. One venturi reduced this annular area to 26 percent of the pipe cross-sectional area (configuration B3), and the other reduced the area to 42 percent (configuration B4).

Comparison of the unshrouded configuration with the configuration having an annular area of 26 percent of the burner cross-sectional area (fig. 12(a)) indicates that at a given pressure ratio the width of the operable band of fuel-air ratios was about the same for both. In terms of pilot-burner air flow, however, the range of operation was smaller for the shrouded configuration (fig. 12(b)). With an inlet pressure of 10 inches of mercury absolute and a pilot-burner air flow of 0.2 pound per second, the operable range of fuel-air ratios was from 0.052 to 0.123 for the unshrouded configuration (B2) and from 0.051 to 0.088 with the shrouded configuration (B3). In other words, the shroud had no effect on the stable range of operation at a given pressure ratio, but it did raise the drag of the burner so that less mass-flow was obtained at a given value of pressure ratio.

Configuration B4 was not investigated under burning conditions, but a cold-flow test indicated that this configuration also had a higher drag than the unshrouded configuration.

Friction-drag coefficients and combustion efficiency. - Cold-flow friction-drag coefficients for several modifications of the parabolic hole-distribution configuration are presented as a function of pressure ratio across the burner in figure 13. The original configuration with the exit annulus open had a drag coefficient of about 4.0 at a pressure ratio of 1.04. Closing the annulus resulted in an increase in drag coefficient to about 4.5. Reducing the annular area at the first row of holes from 50 percent of the cross-sectional area to 42 and 26 percent

of the cross-sectional area resulted in an increase in the drag coefficient to 7.5 and 15.5, respectively, at this pressure ratio. With all configurations, the drag coefficients increased slightly with increasing pressure ratio.

A plot of inlet Mach number against static-pressure ratio for configuration B2, both with and without combustion, is presented in figure 14. Included on this plot are theoretical curves for various drag coefficients and combustor temperature ratios. Because of unreliable heat-balance data, it was impossible to obtain exact values of temperature ratio for the data shown. However, from the values of fuel-air ratio it is believed that the temperature-ratio range was from about 4.0 to 6.5. Comparison of the data with theoretical curves indicates that the values of friction-drag coefficients with burning (when friction drag is defined as total drag minus momentum drag) are about 8.0. Cold-flow friction-drag coefficients for this configuration were between 4 and 5. Other circular configurations also had higher friction-drag coefficients with combustion than under cold-flow conditions.

Combustion efficiency data for the circular pilot burners were somewhat doubtful because of the low values of air flow involved. However, for almost all conditions of inlet pressure, pressure ratio, and fuel-air ratio, the indicated values of efficiency were above 80 percent.

Annular-Segment Pilot Burners

All the annular-segment pilot-burner modifications investigated had parabolic hole-area distributions. The first configuration investigated did not have holes in the sides of the annular segment, and the open-hole area was approximately 84 percent of the pilot-outlet cross-sectional area (configuration AA1). Stability limits of this pilot were not as good as the circular configurations. Considerable flashback occurred at pressure ratios below 1.04, and combustion could not be maintained in the last five stages of the pilot burner at inlet pressures below 13 inches of mercury absolute. The stability limits at an inlet pressure of 13 inches of mercury absolute are presented in figure 15. Combustion efficiencies for various values of pressure ratio and inlet pressure are presented as a function of fuel-air ratio in figure 16. For all conditions investigated, combustion efficiencies obtained were over 80 percent.

The addition of holes along the sides of the annular segment (configuration AA2) increased the operational limits slightly; but the pilot burner still would not operate with inlet pressures below 13 inches of mercury absolute, and flashback still occurred at lower values of pressure ratio.

In an effort to increase the air flow through the first row of holes, scoops were added to all the holes in the first row (fig. 4). This modification resulted in improved operational range and made it possible to operate the burner with inlet pressures as low as 8 inches of mercury absolute. However, flashback was still encountered with pressure ratios below 1.04. In an attempt to eliminate flashback, the fuel-injection station was moved from station 1 to a plane approximately 1 foot upstream of the pilot burner. A sketch of the air-atomizing fuel bar used at this location is presented in figure 5(b). This modification greatly improved the stability at the lower values of pressure ratio. Fuel-air ratio operating limits of this configuration are presented in figure 17. The rich limits shown for inlet pressures of 12 and 30 inches of mercury absolute are fuel-system flow limits, not blow-out or stability limits.

Combustion efficiencies for values of inlet pressure of 10 and 12 inches of mercury absolute and for several pressure ratios are presented as a function of fuel-air ratio in figure 18. The values of combustion efficiency for all conditions are below 80 percent, considerably less than those values obtained with a homogeneous fuel-air mixture. Maximum values of combustion efficiency were obtained near the lean limit, and efficiency decreased with increasing fuel-air ratio. With an inlet pressure of 10 inches of mercury absolute and a pressure ratio of 1.021, the combustion efficiency decreased from approximately 75 to 47 percent, when the fuel-air ratio was increased from 0.043 to 0.092. For a given inlet pressure, the combustion efficiency decreased with increasing pressure ratio (or inlet velocity) across the pilot burner.

The holes in the side of the segment were covered in order to simulate more closely a complete annulus (configuration AA4). The operating range of this configuration was essentially the same as the configuration with the side holes open.

Fuel-system variation. - Operation of configuration AA4 was also investigated with the impinging-jet fuel bars (fig. 5(c)) located 14 and 6 inches upstream of the pilot burner, and with the single-orifice fuel bars (fig. 6) located 15 and 7 inches upstream of the pilot burner. A comparison of the combustion efficiencies obtained with these configurations and with the air-atomizing configuration at inlet pressures between 9.8 and 11.2 inches of mercury absolute and pressure ratios from 1.021 to 1.045 is presented in figure 19. These fuel bars were set at the radial position that gave the highest efficiency at stoichiometric fuel-air ratio. Maximum efficiencies with the air-atomizing and impinging-jet fuel bars were obtained at values of fuel-air ratio between 0.05 and 0.07. With the simple-orifice fuel bars, the efficiency was a maximum near the lean blow-out point and decreased rapidly with increasing fuel-air ratio. With the air-atomizing fuel bar, a maximum efficiency of about 61 percent was obtained at a fuel-air ratio of about 0.06.

The primary objective of these fuel-system changes was to find a configuration which would allow stable operation of the pilot burner over a range of pressure ratios from about 1.02 to 1.10 at pilot-burner-inlet pressures from 10 to 30 inches of mercury absolute. However, it is believed that with a moderate amount of development work, fuel distribution and vaporization could be improved enough to obtain combustion efficiencies over 80 percent, as obtained with the homogeneous fuel-air mixture. It is also probable that the water-quench spray downstream of the pilot burner limits the combustion efficiencies to values considerably below those which could be obtained in an operational installation.

It was noted during the annular-segment pilot-burner investigations that any fuel system which allowed liquid fuel to spray on the outer shroud walls would result in severe flashback and unstable operation. This agrees with the results obtained from the circular pilot-burner investigations.

Friction-drag coefficients. - Cold-flow drag coefficients for various annular configurations varied from about 5.0 to 8.0 (fig. 20). This increase over the values obtained with the best circular pilot-burner configuration is attributed to the reduced ratio of hole area to pilot-burner cross-sectional area in the annular pilot burner. Drag of an annular pilot burner could be reduced by constructing the pilot in a number of segments with holes along the segment sides.

Friction-drag coefficients with combustion were calculated for annular-segment configuration AA3 by subtracting the theoretical values of momentum pressure drop from the measured pressure drop across the pilot. When plotted as a function of inlet Mach number, the values of friction-drag coefficient so calculated showed a considerable amount of scatter. However, most of the values were between 4 and 6. It therefore appears that unlike the circular pilot the friction drag of the annular-segment pilot burner was not higher with combustion than for the cold-flow condition.

CONCLUDING REMARKS

It is possible that coupling effects between the pilot burner and the main combustor might alter the stability characteristics of the pilot burner when it is operating as a component part of a ram-jet combustor. It was impossible to evaluate such effects in the direct-connect rig used. However, the effects of geometric changes in the pilot burner, such as variation of hole-area distribution, addition of scoops, and variation of annular-passage area, should be at least qualitatively applicable to full-scale combustor design. The pilot fuel

system appears to be a critical factor in pilot design with respect to both efficiency and pilot-burner stability. Additional work would be required to obtain the optimum compromise between these two factors for any given installation.

To find the approximate air flow through and pressure ratio across the pilot burner in a given installation, an analysis similar to that of appendix A might be used. This analysis is highly dependent upon assumed pressure losses in the pilot diffuser and in the main stream outside of the pilot, and also upon the ram-jet combustor-inlet-velocity profiles. However, it is probable that the pilot-burner pressure ratio obtained in any practical installation of this type would fall within the range covered in this investigation (1.02 to 1.1). A friction-drag coefficient of about 8.0 appears to be a reasonable value to use in calculations for this type of pilot. Selection of circular or annular cross section would depend on factors such as pilot blockage required, ram-jet-diffuser shape, desired distribution of piloting flame, and length available for pilot installation. For a given amount of pilot blockage, an annular pilot would be shorter and give better distribution of piloting flame. Drag of an annular pilot could be reduced by constructing it in a number of segments with holes along the segment sides, in order to increase the ratio of pilot-burner hole area to blockage area. This segmentation would approach, as a limit, a series of small circular pilots arranged to form an annulus.

SUMMARY OF RESULTS

A 5-inch-diameter circular pilot burner and an annular-segment pilot burner were developed which gave stable operation over a range of fuel-air ratios sufficiently wide for pilot application, with pressure ratios across the pilot from about 1.02 to 1.08, with an inlet pressure of 10 inches of mercury absolute.

Tendency of the circular pilot burners to flashback was reduced by closing the annular gap between the pilot burner and the outer pipe at the outlet end of the pilot. Changing the circular pilot-burner hole-area distribution from parabolic to linear had little effect; however, if addition of fuel-air mixture to the combustion zone is too rapid after the first row of holes, quenching of the flame from the first row can occur. This effect was noted with an annular pilot configuration which would not burn downstream of the first row of holes when the inlet pressure was below 13 inches of mercury absolute. Increasing the flow through the first row by the addition of scoops greatly improved the stability of this burner and made it possible to operate at pressures as low as 8 inches of mercury absolute.

2687 With homogeneous fuel-air mixtures, efficiencies of over 80 percent were obtained with both annular and circular pilots at inlet pressures as low as 10 inches of mercury absolute. With the annular pilot, however, flashback occurred when the pressure ratio across the pilot was below 1.04. Moving the fuel spray to a station approximately 1 foot upstream of the pilot eliminated most of the flashback at the expense of reduced combustion efficiency. It was found in both the circular and annular-segment investigations that severe instability results when liquid fuel is allowed to impinge upon and run down the walls of the inlet ducting.

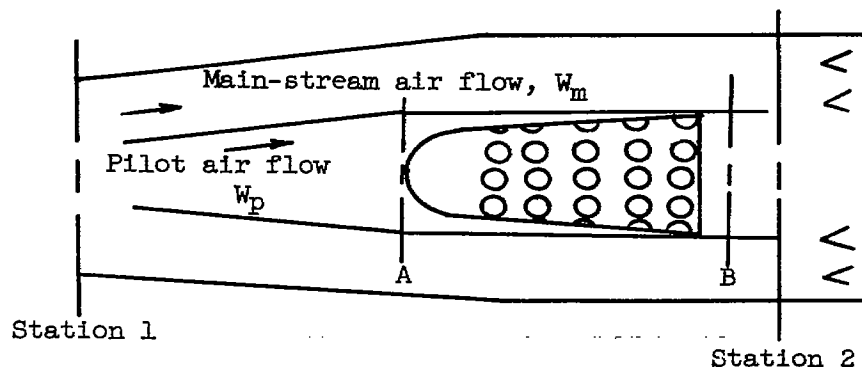
Cold-flow friction-drag coefficient of the best circular pilot burner was about 4.5 with a static-pressure ratio across the pilot of 1.04. With burning, the friction-drag coefficient increased to about 8.0. In order to avoid excessive drag, it was determined that the annular-passage area around the pilot at the first row of holes should be at least one-half the pilot-outlet cross-sectional area. Cold-flow friction-drag coefficients of the annular-segment pilot burners were higher than those of the circular pilot burners because of their reduced ratio of hole area to cross-sectional area. The annular configuration with scoops on the first row of holes and with holes along the segment sides had a cold-flow drag coefficient of 6.5 at a pressure ratio of 1.04.

Lewis Flight Propulsion Laboratory
National Advisory Committee for Aeronautics
Cleveland, Ohio

APPENDIX A

ANALYSIS OF FLOW CONDITIONS

For the calculation of air flow through a low-drag can-type pilot burner, a ram-jet combustor designed for a burner-inlet Mach number of 0.15 (station 2) is considered:



Assumptions made in these calculations are:

(1) Static pressure at the pilot-exhaust station (station 2) is the same for the air flowing through the pilot as for the main-stream air:

$$p_B = (p_2)_m$$

(2) Effects of main-stream and pilot fuel injection are neglected.

(3) Total-pressure loss between stations 1 and 2, outside of the pilot, is 1 percent: $P_2/P_1 = 0.99$.

(4) There is no total-pressure loss in the pilot diffuser: $P_A/P_1 = 1.0$.

(5) Pilot total-temperature ratio T_B/T_A is 4.0.

(6) The cross-sectional area of the pilot is equal to the cross-sectional area at station A: $A_A = A_B = A_p$.

Flow Through Pilot Burner

From conservation of momentum

$$p_A A_p + m_A V_A - C_D A_A q_A = p_B A_p + m_B V_B$$

$$p_B A_p \left(1 + \gamma M_A^2 - \frac{C_D}{2} \gamma M_A^2 \right) = p_B A_p (1 + \gamma_B M_B^2)$$

Dividing by $p_A A_p$

$$1 + \gamma M_A^2 \left(1 - \frac{C_D}{2} \right) = \frac{p_B}{p_A} (1 + \gamma_B M_B^2) \quad (1)$$

Also

$$W = g \rho A V = \frac{p}{Rt} A M \sqrt{\gamma g R t} = p A M \sqrt{\frac{\gamma g}{R t}}$$

And for $M < 0.2$,

$$W = p A M \sqrt{\frac{\gamma g}{R t}}$$

(assuming negligible difference between static and total temperature).

Also

$$W_A^2 = W_B^2$$

and

$$\frac{M_A^2 p_A^2 \gamma_A}{T_A} = \frac{M_B^2 p_B^2 \gamma_B}{T_B}$$

and then

$$\gamma_B M_B^2 = \gamma_A M_A^2 \frac{p_A^2}{p_B^2} \frac{T_B}{T_A}$$

Substituting in equation (1)

$$1 + \gamma_A M_A^2 \left(1 - \frac{C_D}{2} \right) = \frac{p_B}{p_A} \left[1 + \left(\frac{p_A}{p_B} \right)^2 \frac{T_B}{T_A} \gamma_A M_A^2 \right]$$

Then

$$\gamma M_A^2 \left(\frac{C_D}{2} - 1 + \frac{P_A}{P_B} \frac{T_B}{T_A} \right) = 1 - \frac{P_B}{P_A} \quad (2)$$

Also

$$\left(\frac{P_B}{P_A} \right) \left(\frac{P_A}{P_1} \right) = \frac{P_B}{P_1} \quad (3)$$

where $\frac{P_A}{P_1} = f(M_A)$ and $P_1 = P_A$.

From equation (2), values of M_A were calculated for values of P_B/P_A between 0.96 and 1.0 and values of C_D from 4.0 to 24.0 with $T_B/T_A = 4.0$. Corresponding values of P_B/P_1 were calculated from equation (3). Curves showing the variation of P_B/P_1 with M_A for various values of C_D when $T_B/T_A = 4.0$, are plotted in figure 21.

Flow Around Pilot

Since

$$W = \rho_0 A V = p A M \sqrt{\frac{\gamma g}{R t}}$$

if total values are substituted for static values of pressure and temperature,

$$W = \frac{P_A \sqrt{\gamma g} M}{\sqrt{R T} \left(1 + \frac{\gamma - 1}{2} M^2 \right)^{\frac{\gamma + 1}{2(\gamma - 1)}}} = \frac{0.918 P A M}{\sqrt{T} (1 + 0.2 M^2)^3}$$

for $\gamma = 1.4$, then

$$\frac{W \sqrt{T}}{0.918 P A} = \frac{M}{(1 + 0.2 M^2)^3}$$

With no pilot, $M_2 = 0.15$ and $\frac{W_2 \sqrt{T_2}}{0.918 P_2 A_2} = 0.148 = \frac{W_1 \sqrt{T_1}}{0.918 P_2 A_2}$. With a pilot installed, Mach number of the main-stream air at station 2 for various values of pilot air flow W_p/W_1 and pilot blockage A_p/A_2 can be determined from

$$\left[\frac{M_2}{(1 + 0.2M_2^2)^3} \right]_m = \frac{\left(\frac{W_1 - W_p}{W_1} \right)}{\left(\frac{A_2 - A_p}{A_2} \right)} \left(\frac{W_1 \sqrt{T_1}}{0.918 P_2 A_2} \right) = \frac{\left(1 - \frac{W_p}{W_1} \right)}{\left(1 - \frac{A_p}{A_2} \right)} (0.148) \quad (4)$$

Also

$$\left(\frac{P_2}{P_1} \right)_m = 0.99 \left(\frac{P_2}{P_2} \right)_m$$

where

$$\left(\frac{P_2}{P_2} \right)_m = f(M_2)_m \quad (5)$$

Likewise, the Mach number at station A in the pilot can be determined for various values of pilot air flow and pilot blockage from

$$\begin{aligned} \frac{M_A}{(1 + 0.2M_A^2)^3} &= \frac{W_p \sqrt{T_A}}{(0.918) P_A A_p} = \frac{W_p \sqrt{T_1}}{(0.918) P_1 A_p} = \frac{\left(\frac{W_p}{W_1} \right)}{\left(\frac{P_1}{P_2} \right) \left(\frac{A_p}{A_2} \right)} \left(\frac{W_1 \sqrt{T_1}}{0.918 P_2 A_2} \right) \\ &= \frac{\left(\frac{W_p}{W_1} \right)}{\left(\frac{P_1}{P_2} \right) \left(\frac{A_p}{A_2} \right)} (0.148) \end{aligned} \quad (6)$$

From equation (4), values of $(M_2)_m$ were calculated with assumed values of A_p/A_2 from 0.05 to 0.25 and assumed values of $(W_p/W_1)/(A_p/A_2)$ from 0.2 to 0.6. Corresponding values of $(p_2/P_1)_m$ and M_A were calculated with equation (5) and equation (6), respectively. Curves showing

the variation of $(p_2/P_1)_m$ with M_A or with $(W_p/W_1)/(A_p/A_1)$ for values of A_p/A_2 from 0.05 to 0.25 are also plotted in figure 21. The points of intersection of these curves with those which show variation of p_B/P_1 with M_A for various values of C_D are points at which the assumed outlet condition $p_B = (p_2)_m$ is satisfied for the given conditions. A cross plot of these intersection points, showing variation of $(W_p/W_1)/(A_p/A_2)$ with A_p/A_2 for various values of C_D is presented in figure 22.

It can be seen in figure 22 that with a pilot drag coefficient of 8, the ratio of pilot air-flow ratio to pilot blockage ratio varies from about 0.34 to 0.375 as pilot blockage ratio varies from 0.05 to 0.25.

APPENDIX B

SYMBOLS

The following symbols were used in this report:

A	area, sq ft
C_D	friction-drag coefficient
f/a	fuel-air ratio
g	acceleration due to gravity, 32.2 ft/sec ²
H	enthalpy, Btu/lb
M	Mach number
m	mass flow, slugs/sec
P	stagnation pressure
p	static pressure
q	dynamic pressure
R	gas constant
T	stagnation temperature, °R
t	static temperature, °R
V	velocity, ft/sec
W	weight flow, lb/sec
γ	ratio of specific heats
η_b	combustion efficiency, percent
ρ	mass density

Subscripts:

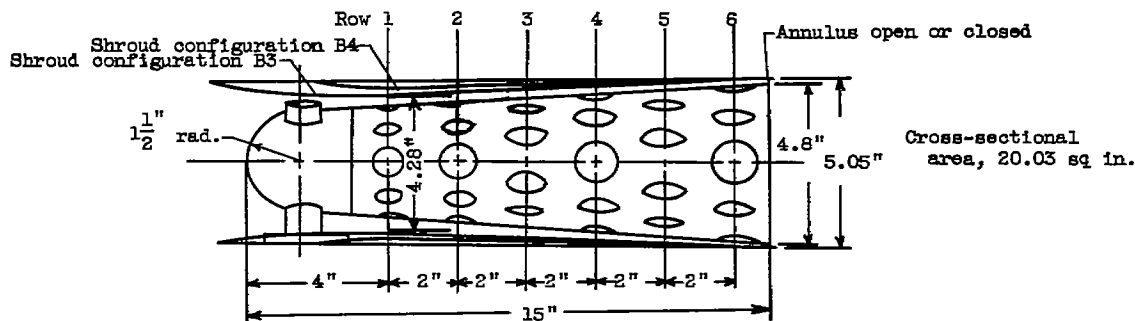
a	air
e	exhaust-gas cooling-water spray

- f fuel
- g gas (mixture of air and fuel at station 2 and exhaust products at stations 3 or 4, fig. 1)
- i in
- j water-jacket cooling water
- m main stream
- o out
- p pilot burner
- s steam
- w water
- 1 upstream fuel-injection station (fig. 1)
- 2 pilot-burner inlet (fig. 1)
- 3 pilot-burner outlet (fig. 1)
- 4 exhaust-gas temperature survey station (fig. 1)

REFERENCES

1. Shillito, T. B., and Nakanishi, Shigeo: Effect of Design Changes and Operating Conditions on Combustion and Operational Performance of a 28-Inch Diameter Ram-Jet Engine. NACA RM E51J24, 1952.
2. Bennet, W. J., and Maloney, J: Altitude Tests of the Convair 20 Inch Diameter Can Type Combustor. Rep. No. ZM-9136-010, Consolidated Vultee Aircraft Corp., San Diego (Calif.), May 10, 1950.
3. Longwell, J. P., Weiss, M. A., and Van Sweringen, R. A., Jr.: Report on Design Variables in Small-Scale Ram-Jet Altitude Pilots. Rep. No. PDN 5582, Esso Lab., Process Div., Standard Oil Development Co., Jan. 9, 1951. (Contract NOrd-9233, SOD/CM 656.)

TABLE I - CIRCULAR PILOT CONFIGURATIONS



Configuration A: First row of holes only; exit annulus open.

A1: Six 3/4-in.-diam. holes; total open hole area 2.650 sq in.

A2: Nine 1/2-in.-diam. holes; total open hole area 1.767 sq in.

A3: Eighteen 1/4-in.-diam. holes; total open hole area 0.883 sq in.

Configuration B: Six-row pilot with parabolic hole-area distribution. Total open hole area 121.7 percent of cross-sectional area.

Row	1	2	3	4	5	6
No. of holes	9	8	8	8	8	8
Hole diam. (in.)	1/2	5/8	3/4	7/8	15/16	1

B1: Exit annulus open.

B2: Exit annulus closed.

B3: Exit annulus closed; shroud incorporated to reduce annular area at first row of holes to 26 percent of pilot-outlet area.

B4: Exit annulus closed; shroud incorporated to reduce annular area at first row of holes to 42 percent of pilot-outlet area.

Configuration C: Six-row pilot with linear hole-area distribution. Total open hole area 120.6 percent of cross-sectional area.

Row	1	2	3	4	5	6
No. of holes	9	8	8	8	8	8
Hole diam. (in.)	1/2	4-13/16 and 4-7/8 holes alternating				

C1: Exit annulus open.

C2: Exit annulus closed.

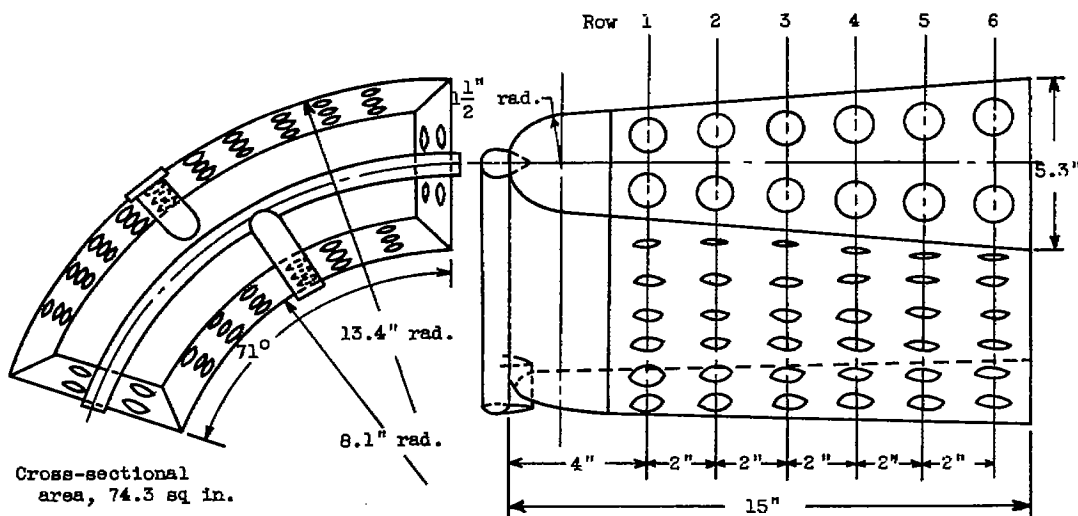
C3: Exit annulus closed; thimbles on six first-row holes and three second-row holes (fig. 11).

Configuration D: Six-row pilot with parabolic hole distribution; exit annulus closed; total open hole area 126.1 percent of cross-sectional area.

Row	1	2	3	4	5	6
No. of holes	6	8	8	8	8	8
Hole diam. (in.)	3/4	5/8	3/4	7/8	15/16	1



TABLE II - ANNULAR-SEGMENT PILOT CONFIGURATIONS



Configuration AAl: Exit annulus closed; no holes in sides; total open hole area 84.0 percent of cross-sectional area.

Row		1	2	3	4	5	6
Top surface	No. of holes	10	10	10	10	10	10
	Hole diam. (in.)	5/8	3/4	7/8	1	1	1
Bottom surface	No. of holes	6	6	6	6	6	6
	Hole diam. (in.)	11/16	13/16	15/16	1 1/16	1 1/16	1 1/16

Configuration AA2: Exit annulus closed; top and bottom surface holes same as in configuration AAl; total open hole area 103.9 percent of cross-sectional area.

Row		1	2	3	4	5	6
Side surfaces	No. of holes in each side	2	2	2	2	2	2
	Hole diam. (in.)	5/8	3/4	7/8	1	1	1



Configuration AA3: Same as configuration AA2 but with scoops on first row of holes. See figure 4.

Configuration AA4: Same as configuration AAl but with scoops on first row of holes.

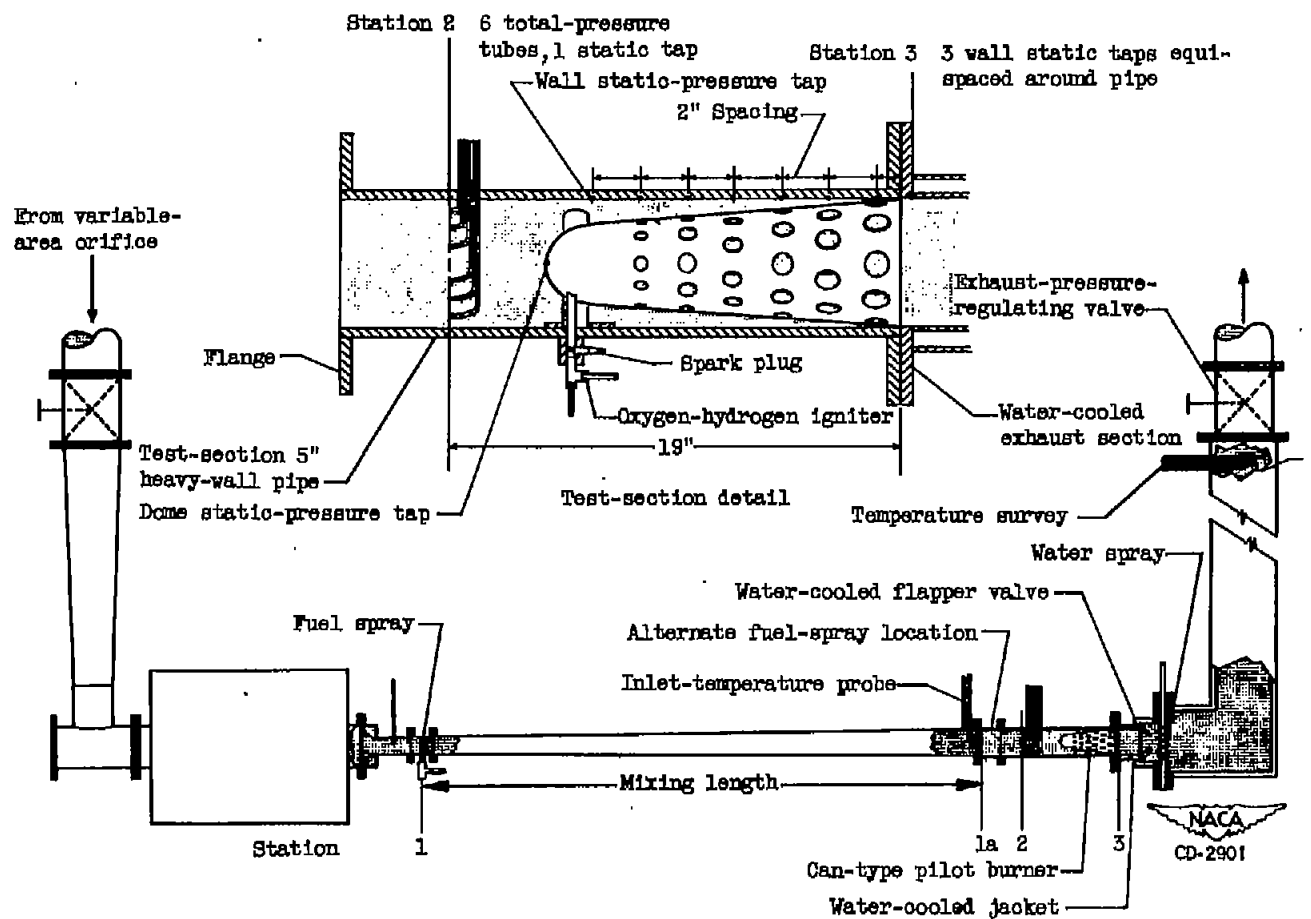


Figure 1. - Test rig for circular pilot-burner investigation.

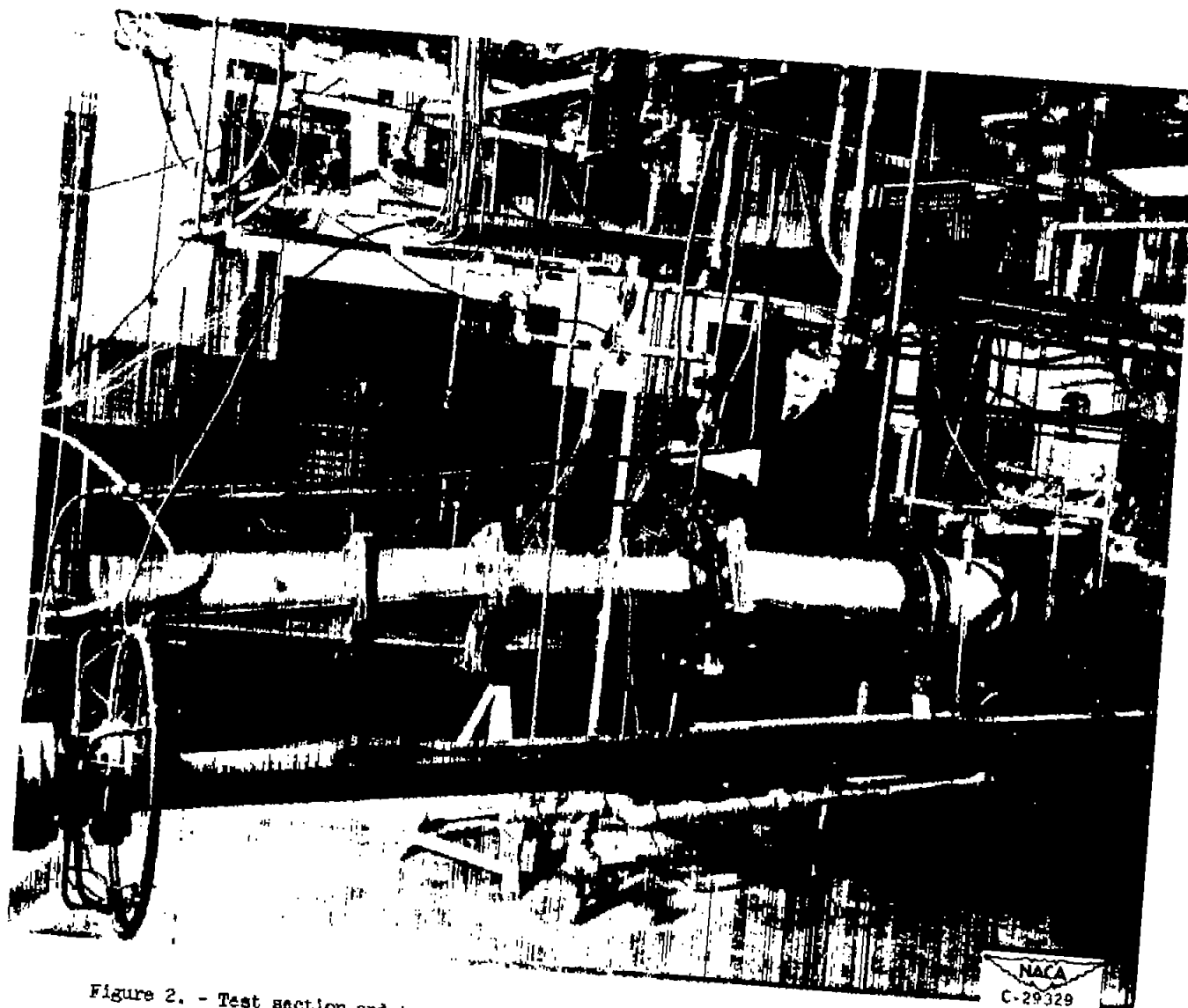


Figure 2. - Test section and transition section used in annular-segment pilot-burner tests.

NACA RM E52023

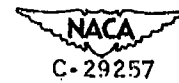
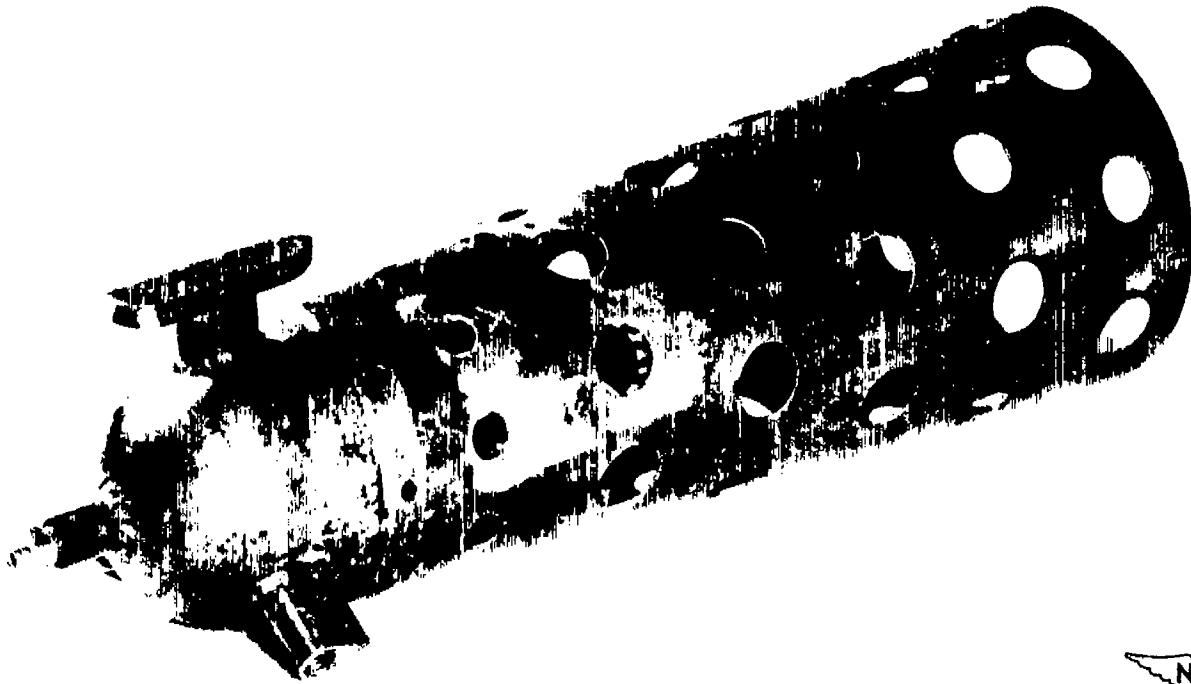


Figure 3. - Typical multirow circular pilot burner.

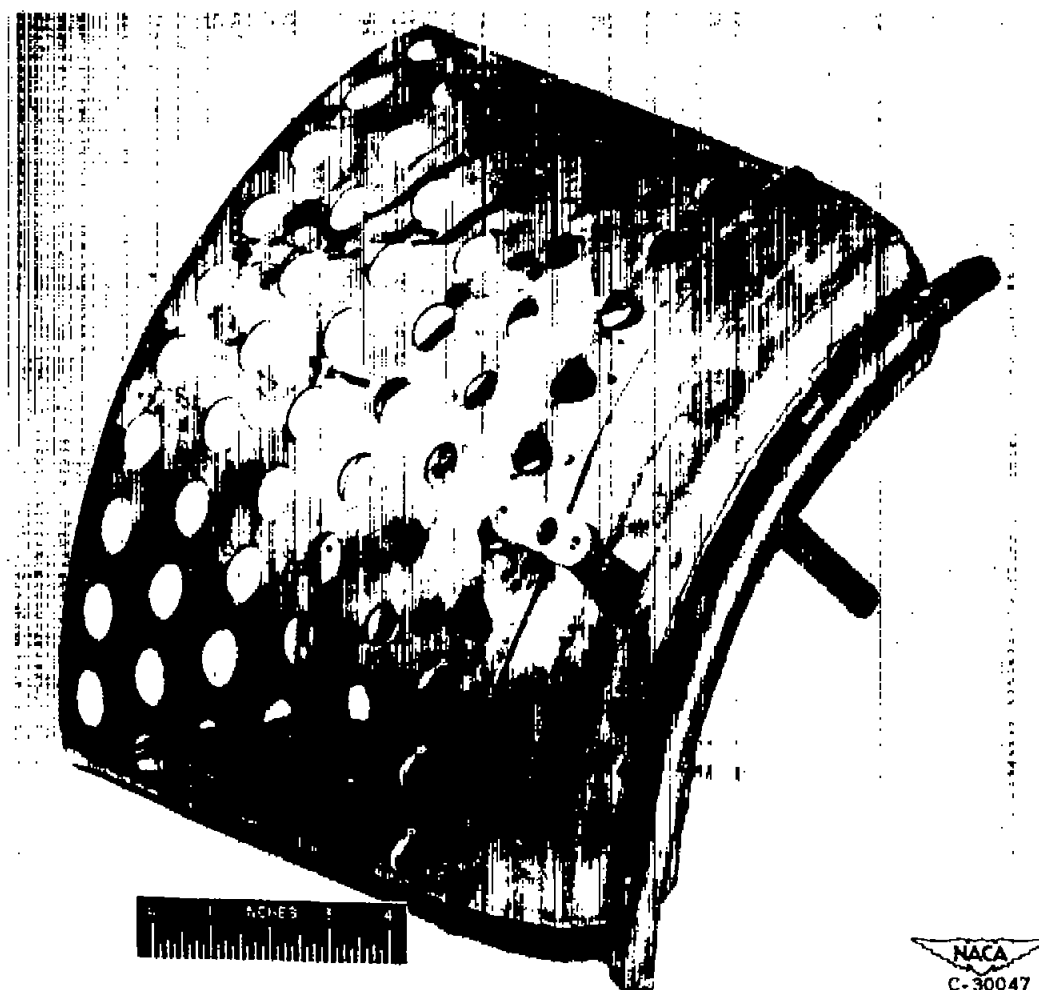
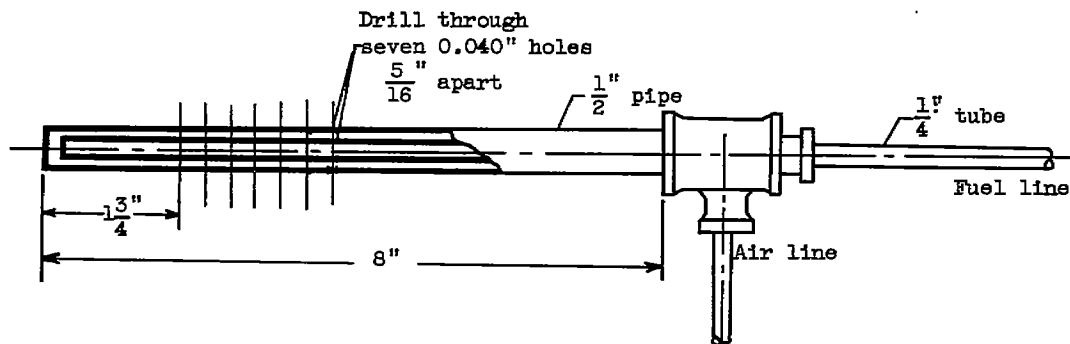
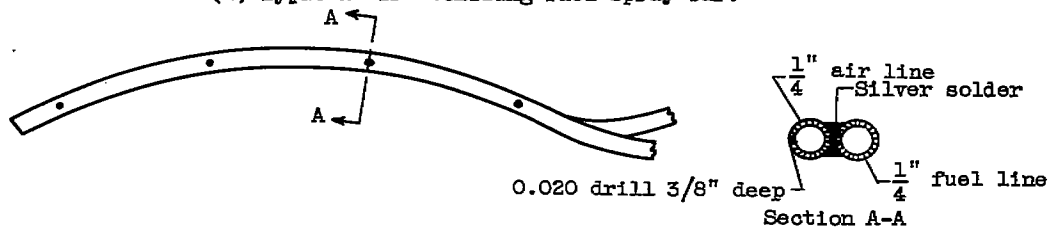


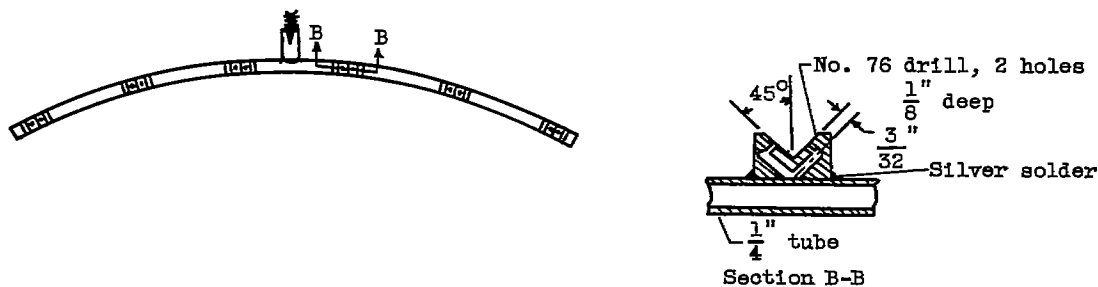
Figure 4. - Typical annular-segment pilot burner.



(a) Typical air-atomizing fuel spray bar.



(b) Air-atomizing fuel spray bar used to inject fuel 12 inches upstream of annular-segment pilot burner.



(c) Impinging-jet fuel spray bar.

Figure 5. - Fuel spray bar details.



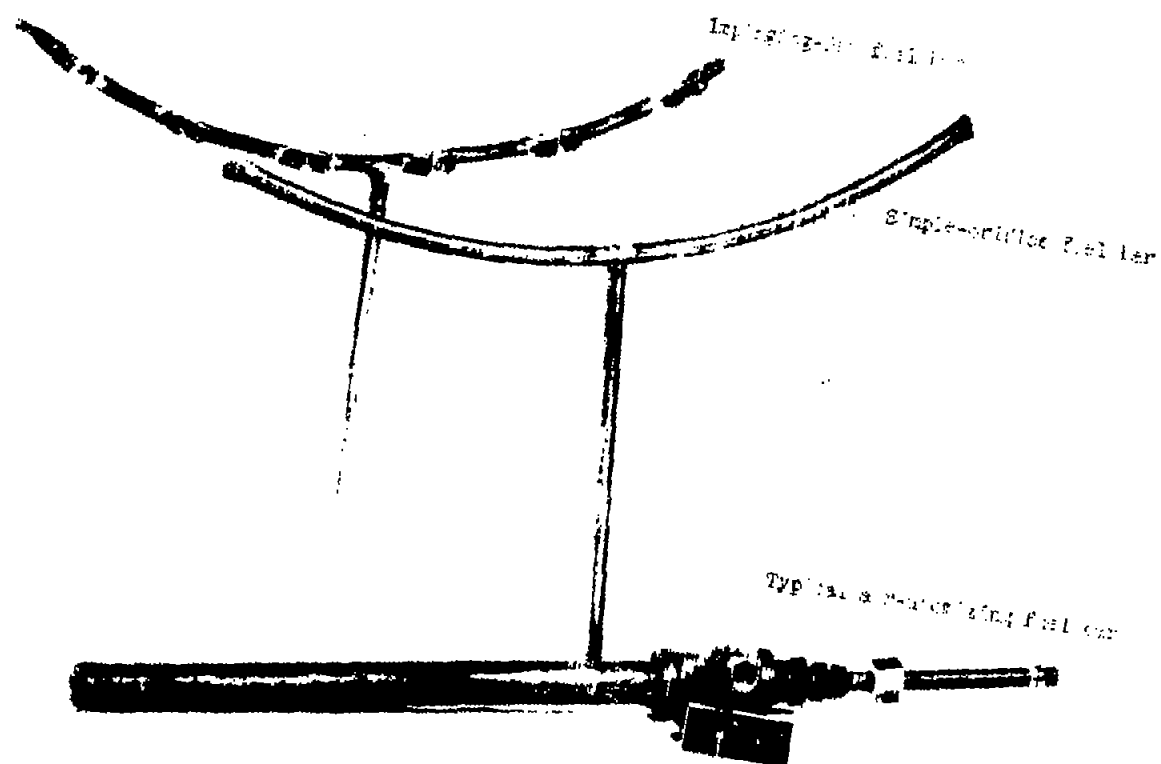


Figure 6. - Several types of fuel spray bar used in pilot-burner investigations.



NACA RM ES2J23

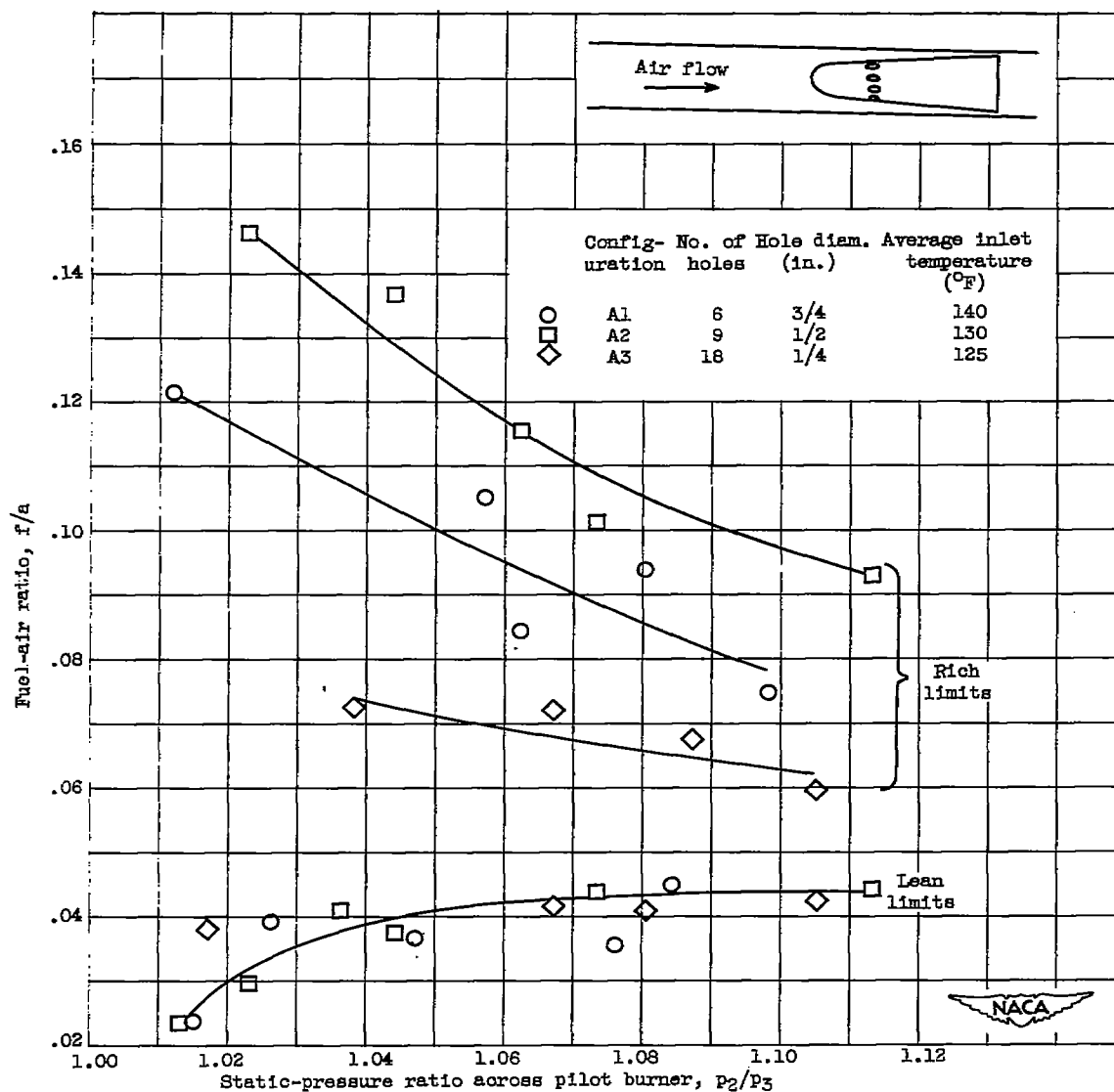


Figure 7. - Effect of first-row hole diameter on blow-out limits. Single-row pilot burner. Inlet pressure, 20 inches of mercury absolute; homogeneous fuel-air mixture.

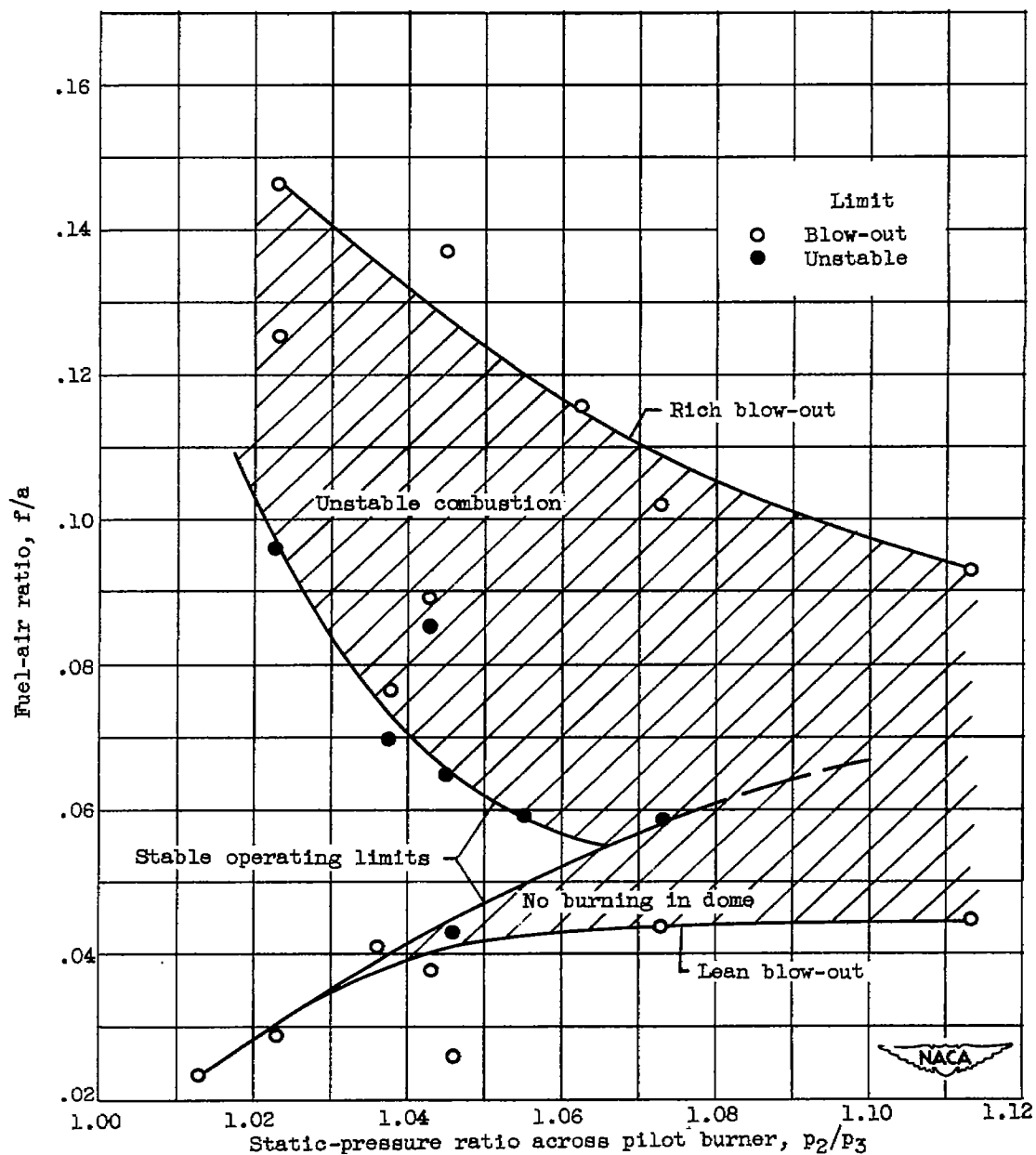


Figure 8. - Stable operation and blow-out limits (configuration A2). Single-row pilot burner with nine 1/2-inch-diameter holes. Inlet pressure, 20 inches of mercury absolute; homogeneous fuel-air mixture; average inlet temperature, 130° F.

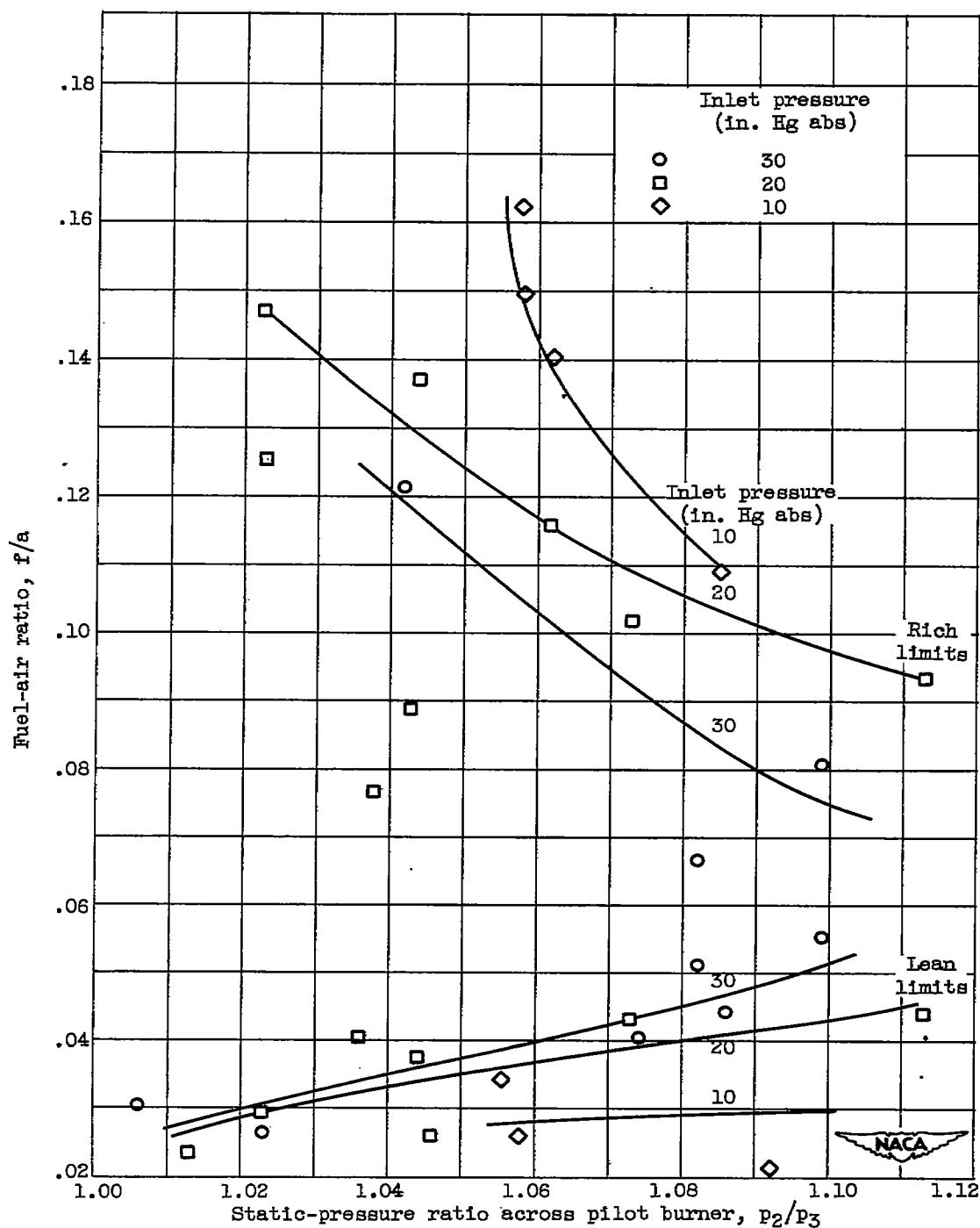


Figure 9. - Effect of inlet pressure on blow-out limits. Single-row pilot burner with nine 1/2-inch-diameter holes (configuration A2). Homogeneous fuel-air mixture; average inlet temperature, 130° F.

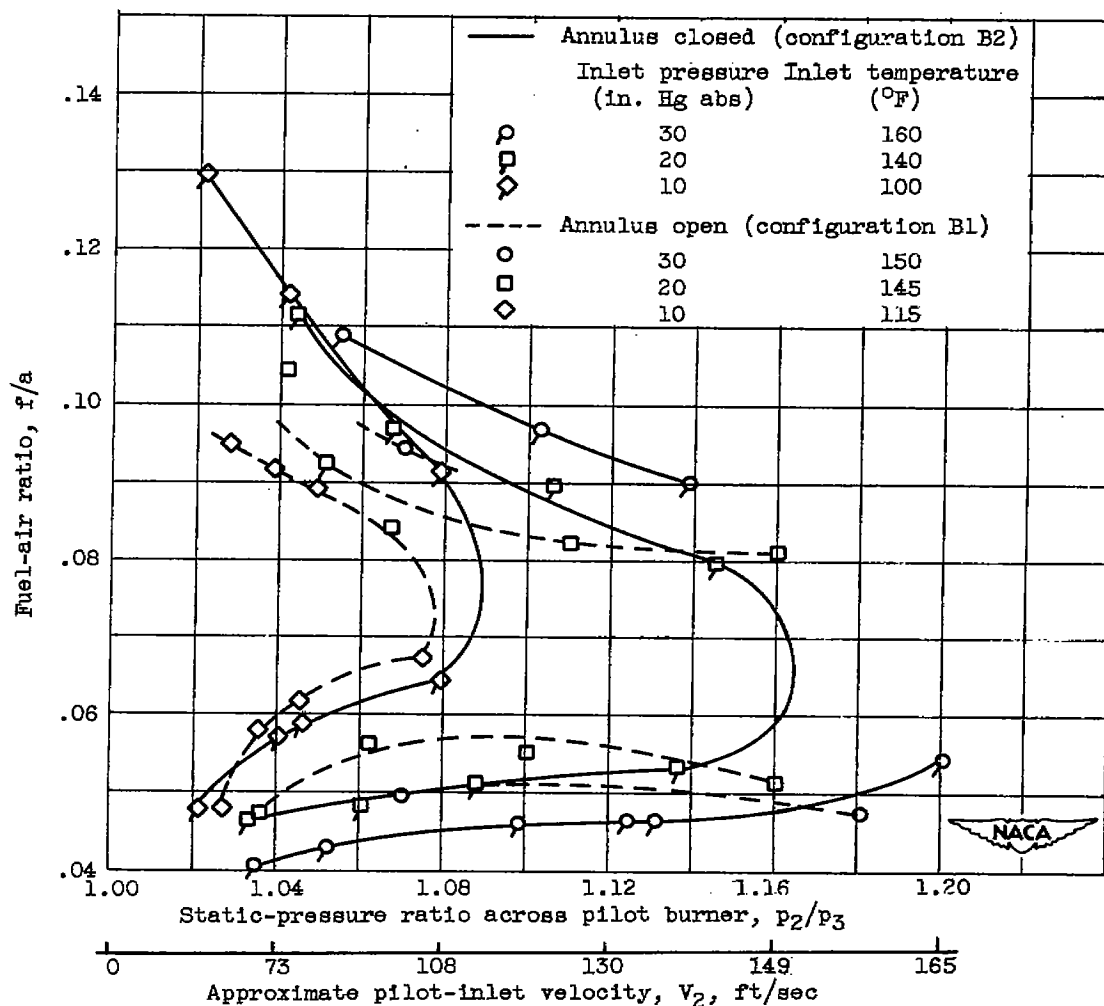
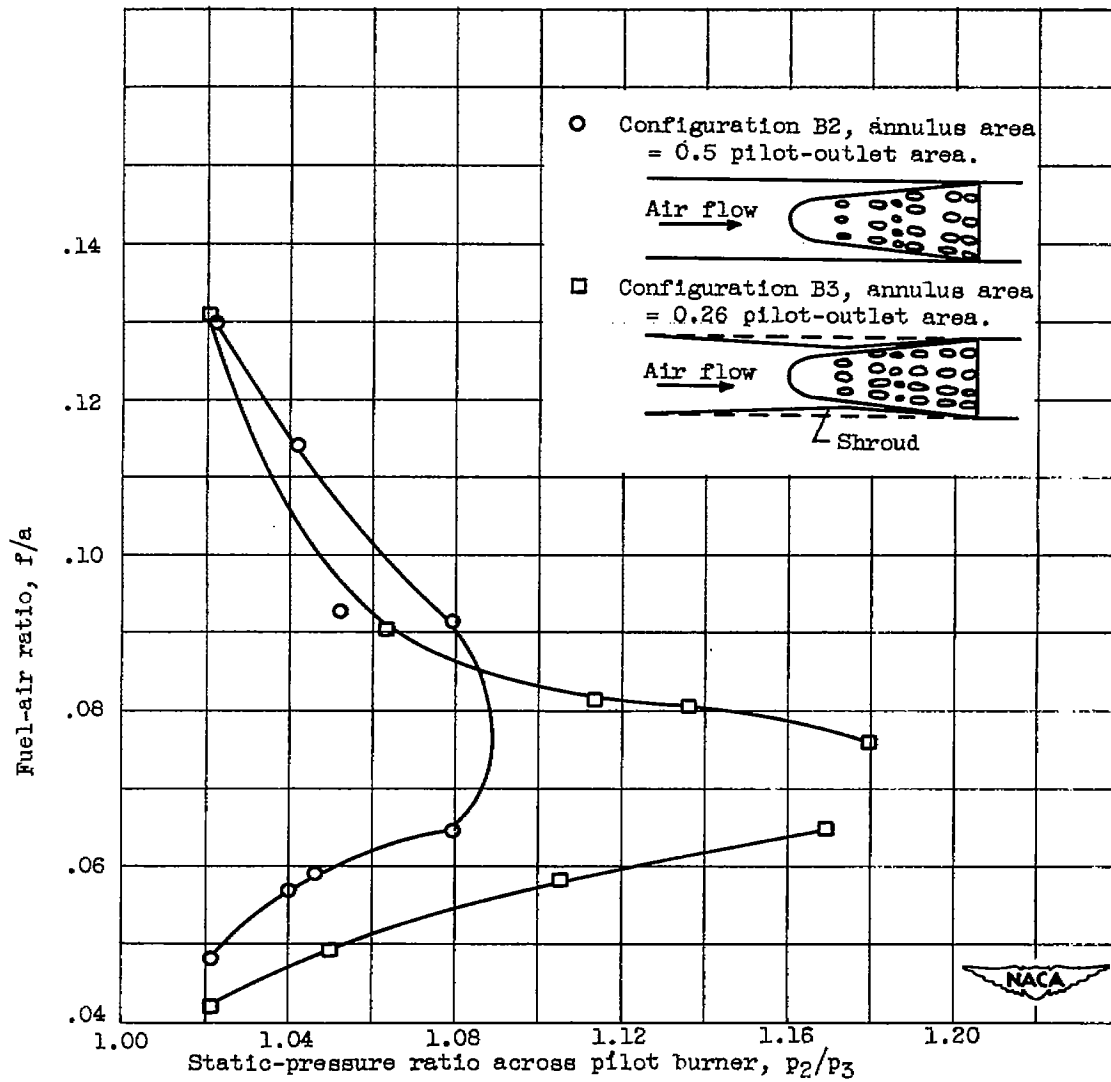


Figure 10. - Effect of annulus opening at pilot-burner outlet on stability limits. Six-row pilot burner with parabolic hole-area distribution. Homogeneous fuel-air mixture.

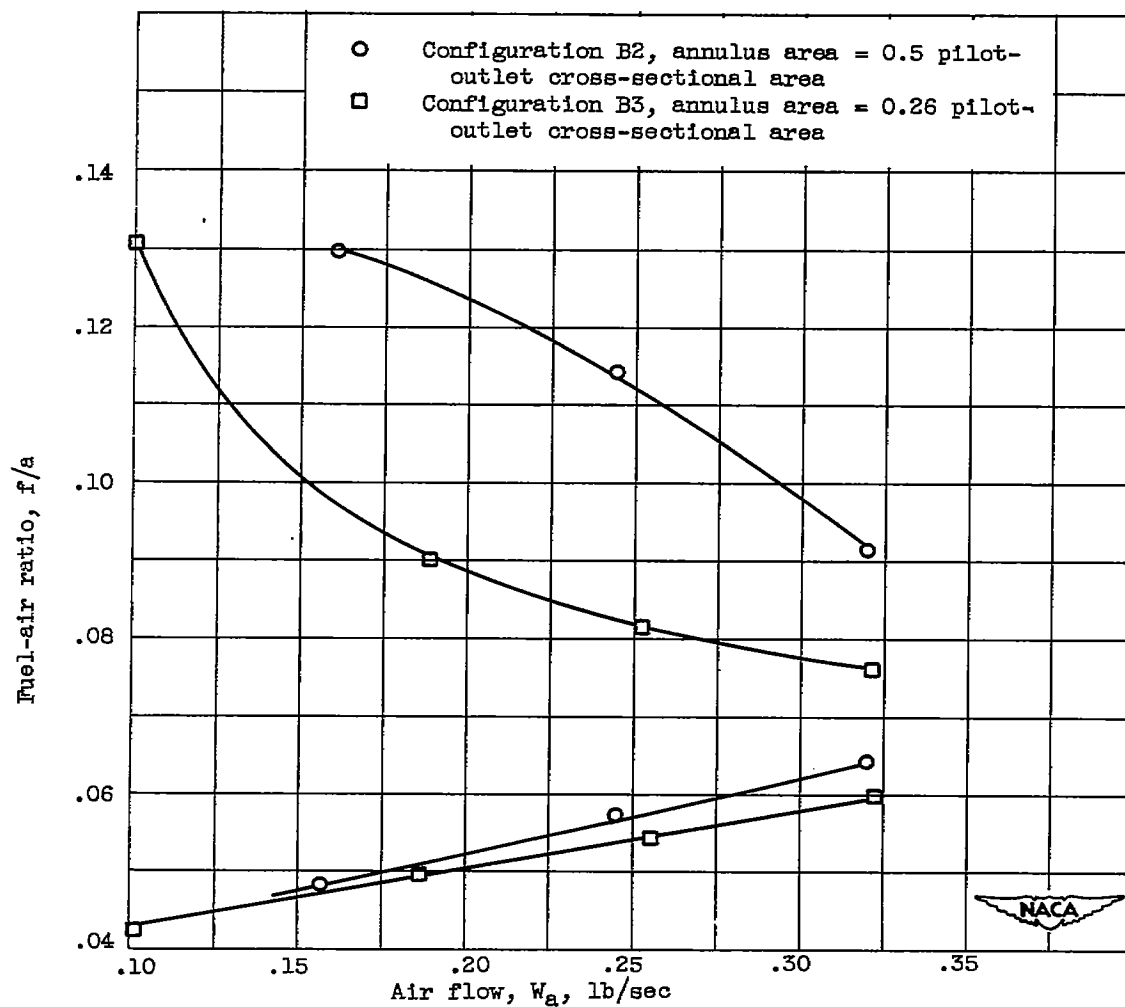


Figure 11. - Pilot-burner interior showing "thimbles" on first- and second-row holes.



(a) Stability limits as function of static-pressure ratio across pilot burner.

Figure 12. - Effect of annular shroud area on pilot-burner stability limits. Six-stage pilot burner with parabolic hole-area distribution. Homogeneous fuel-air mixture. Inlet pressure, 10 inches of mercury absolute.



(b) Stability limits as function of air flow.

Figure 12. - Effect of annular shroud area on pilot-burner stability limits. Six-stage pilot burner with parabolic hole-area distribution. Homogeneous fuel-air mixture. Inlet pressure, 10 inches of mercury absolute.

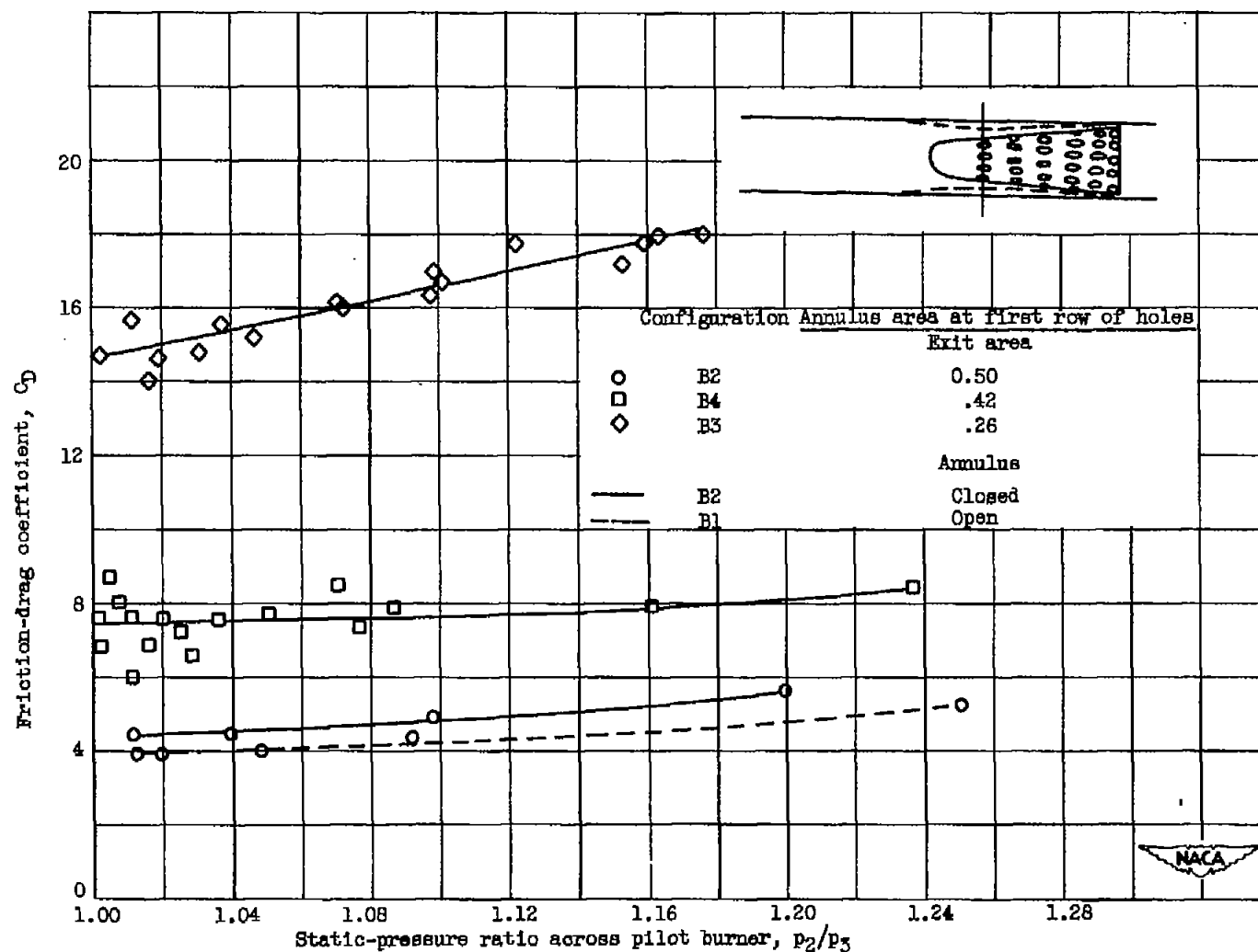


Figure 13. - Effect of static-pressure ratio and configuration changes on isothermal friction drag of pilot burner with six-row parabolic hole-area distribution.

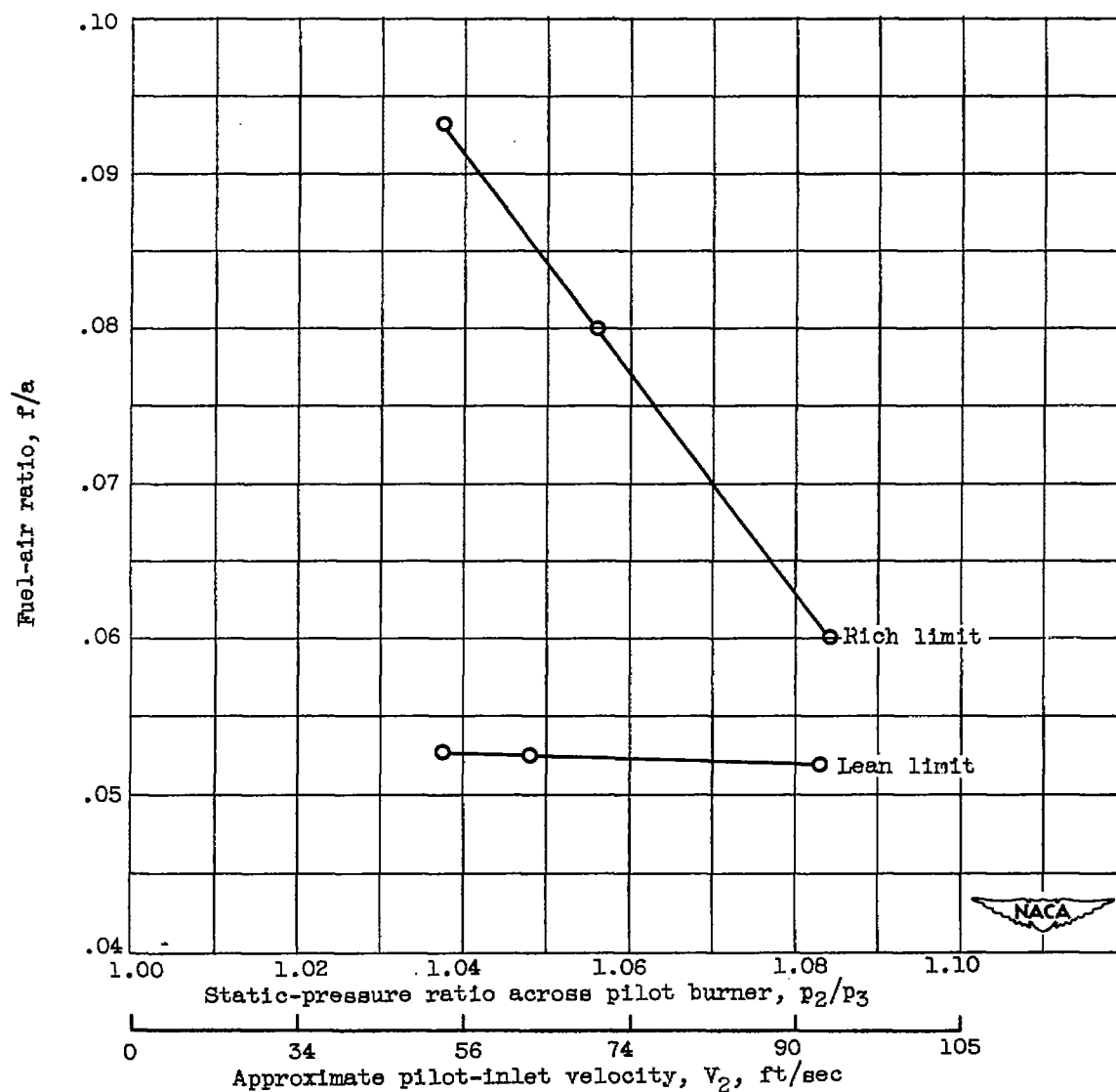


Figure 15. - Effect of static-pressure ratio or inlet velocity on stability limits of annular-segment pilot (configuration AA1). Inlet pressure, 13 inches of mercury absolute; homogeneous fuel-air mixture; average inlet temperature, 185° F.

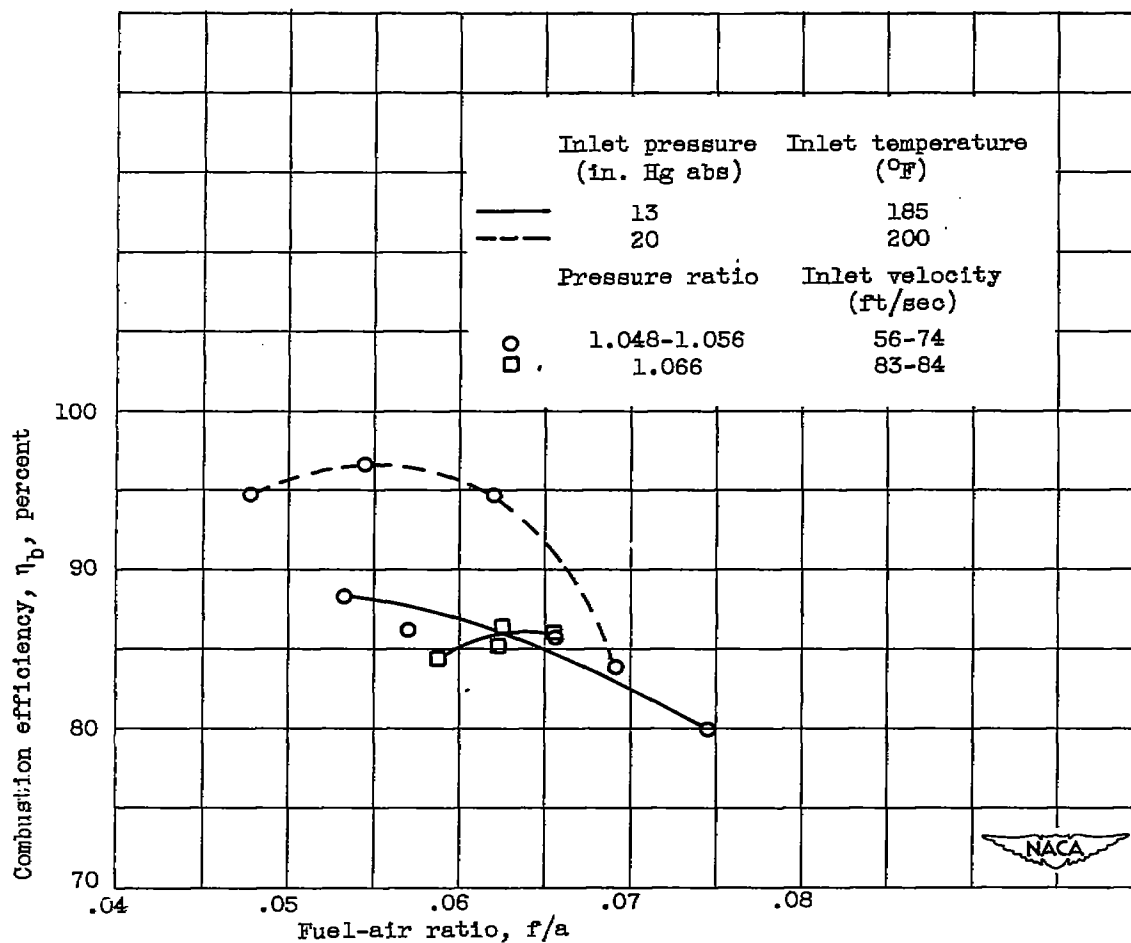


Figure 16. - Effect of fuel-air ratio and operating conditions on combustion efficiency. Annular-segment pilot burner. Configuration AAl. Homogeneous fuel-air mixture.

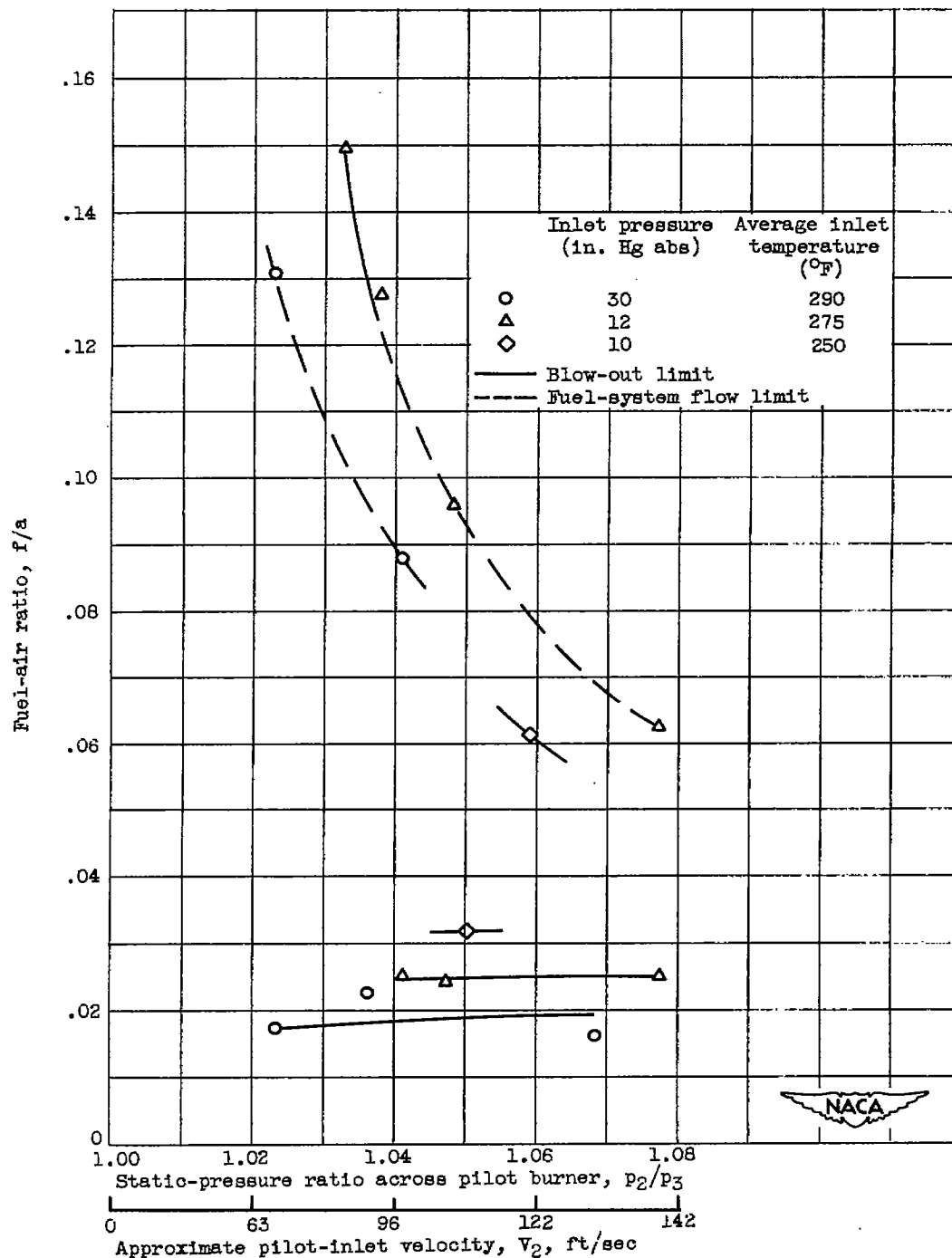


Figure 17. - Effect of static-pressure ratio or inlet velocity on stability limits of annular-segment pilot burner. Configuration AA3. Fuel injected (12 in. upstream of pilot burner) with air-atomizing fuel bars.

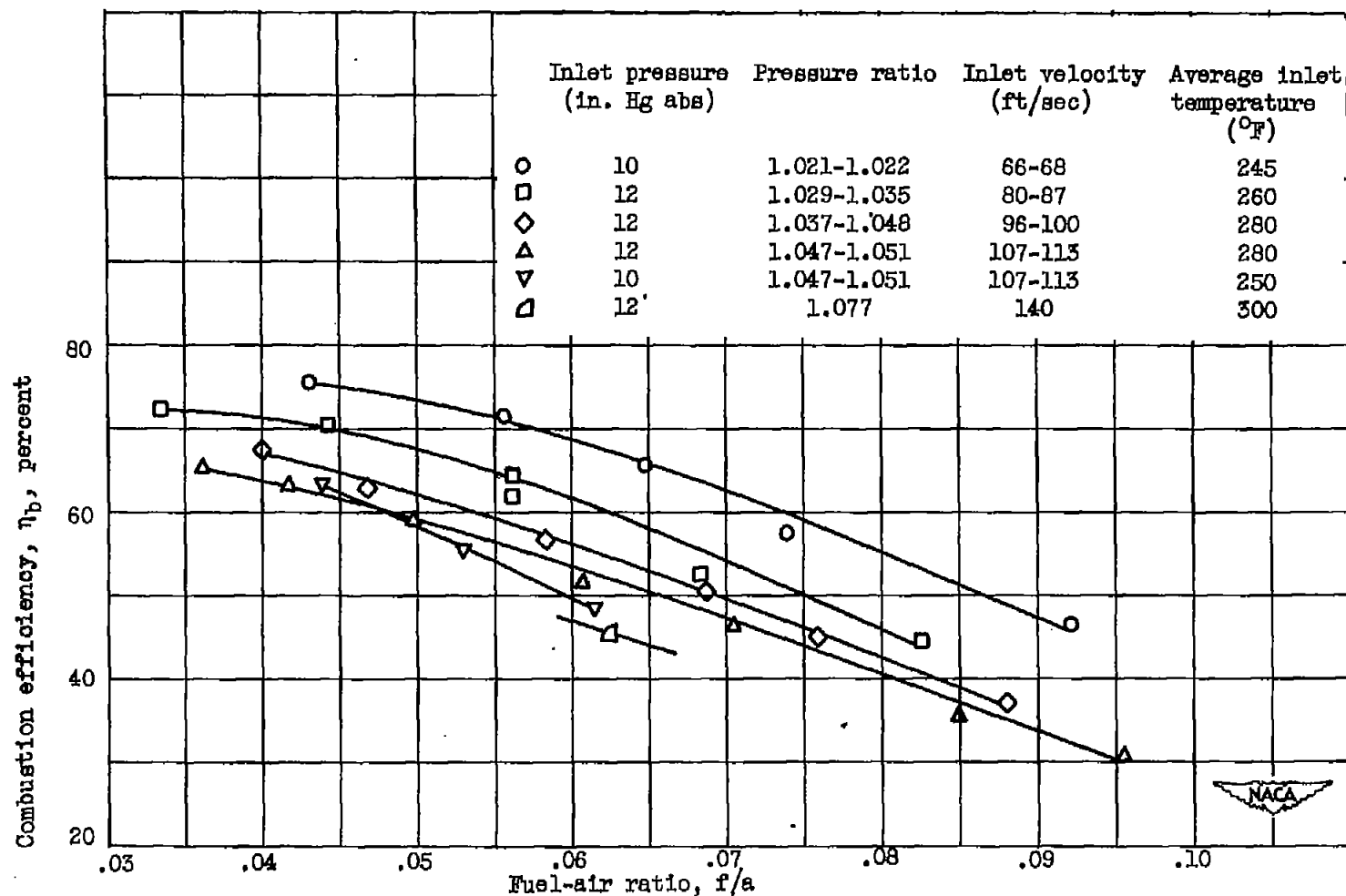


Figure 18. - Variation of combustion efficiency with fuel-air ratio for several values of static-pressure ratio or inlet velocity. Annular-segment pilot configuration AA3. Fuel injected 12 inches upstream of pilot burner with air-atomizing fuel bars. Inlet pressure, 10 inches of mercury absolute.

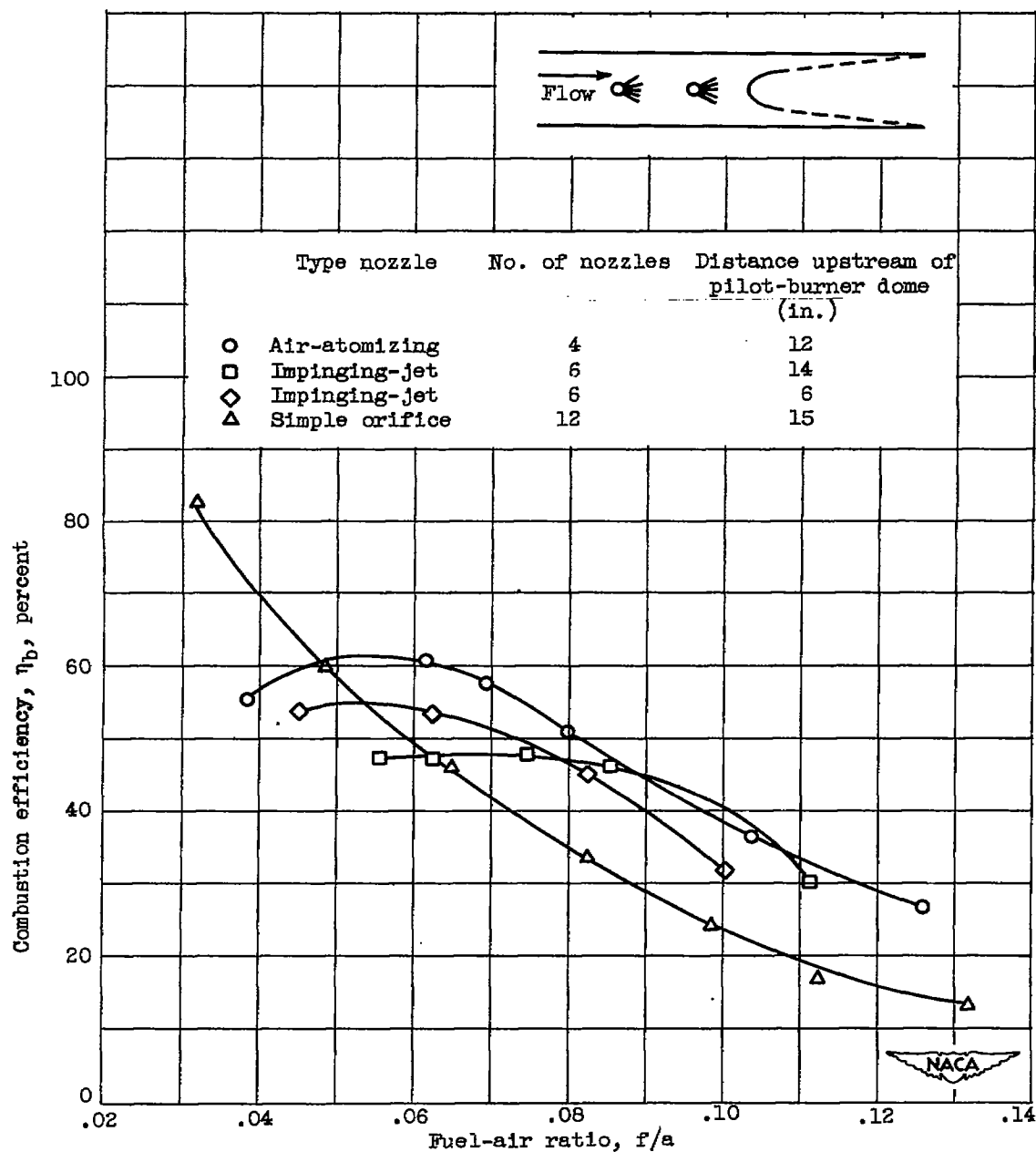


Figure 19. - Effect of fuel-nozzle type and longitudinal position on combustion efficiency over a range of fuel-air ratios. Inlet pressure, 9.8 to 11.2 inches of mercury absolute; pressure ratio across pilot burner, 1.021 to 1.045; inlet velocity 65 to 75 feet per second; average inlet temperature, 200° F; annular-segment pilot, configuration AA4.

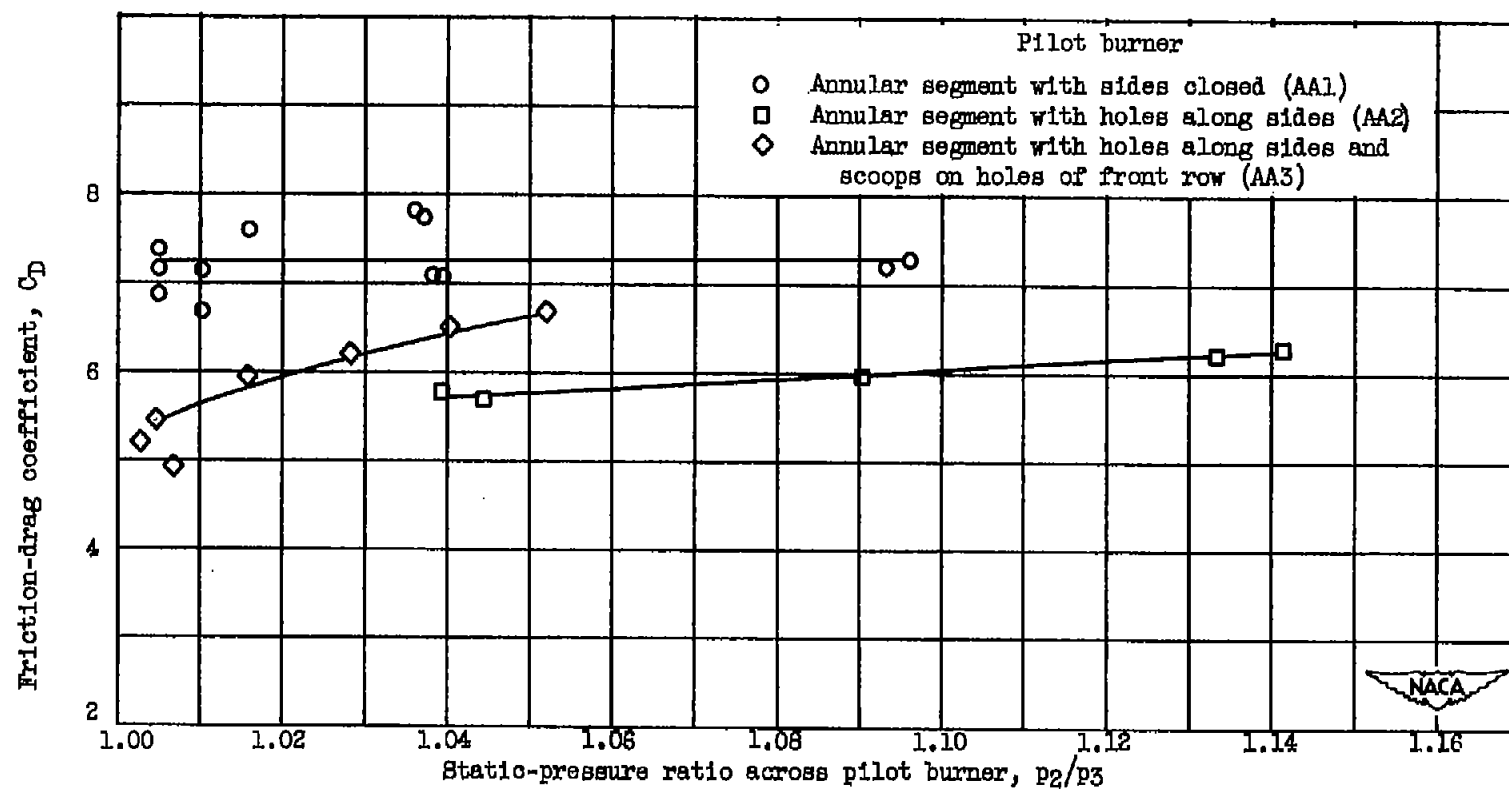


Figure 20. - Friction-drag coefficients for three annular-segment pilot burners. Isothermal flow.

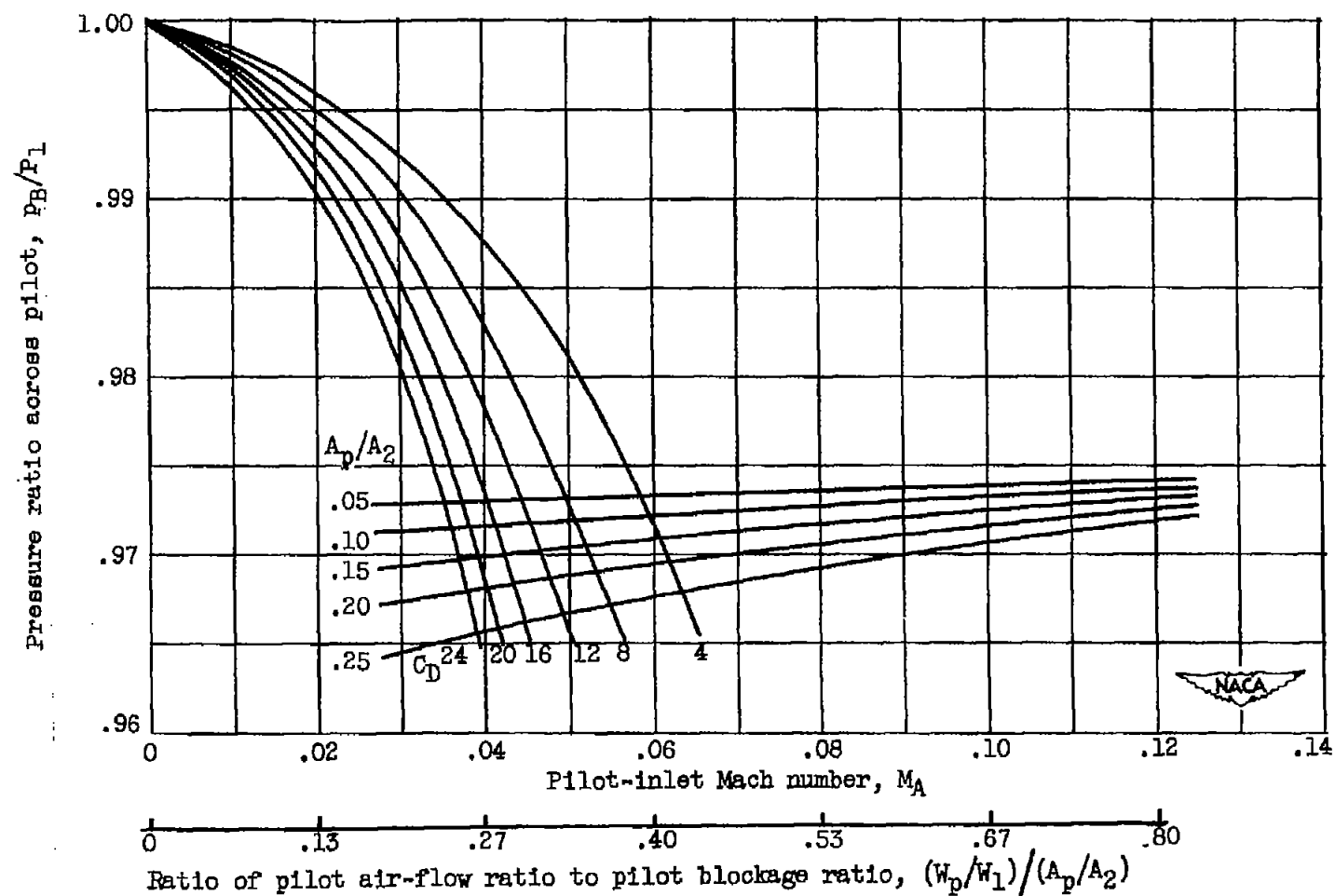


Figure 21. - Variation of pressure ratio across pilot with pilot-inlet Mach number for various values of pilot drag coefficient and pilot blockage. Pilot temperature ratio, 4.0; burner design inlet Mach number, 0.15; burner-inlet-diffuser pressure recovery, 0.99.

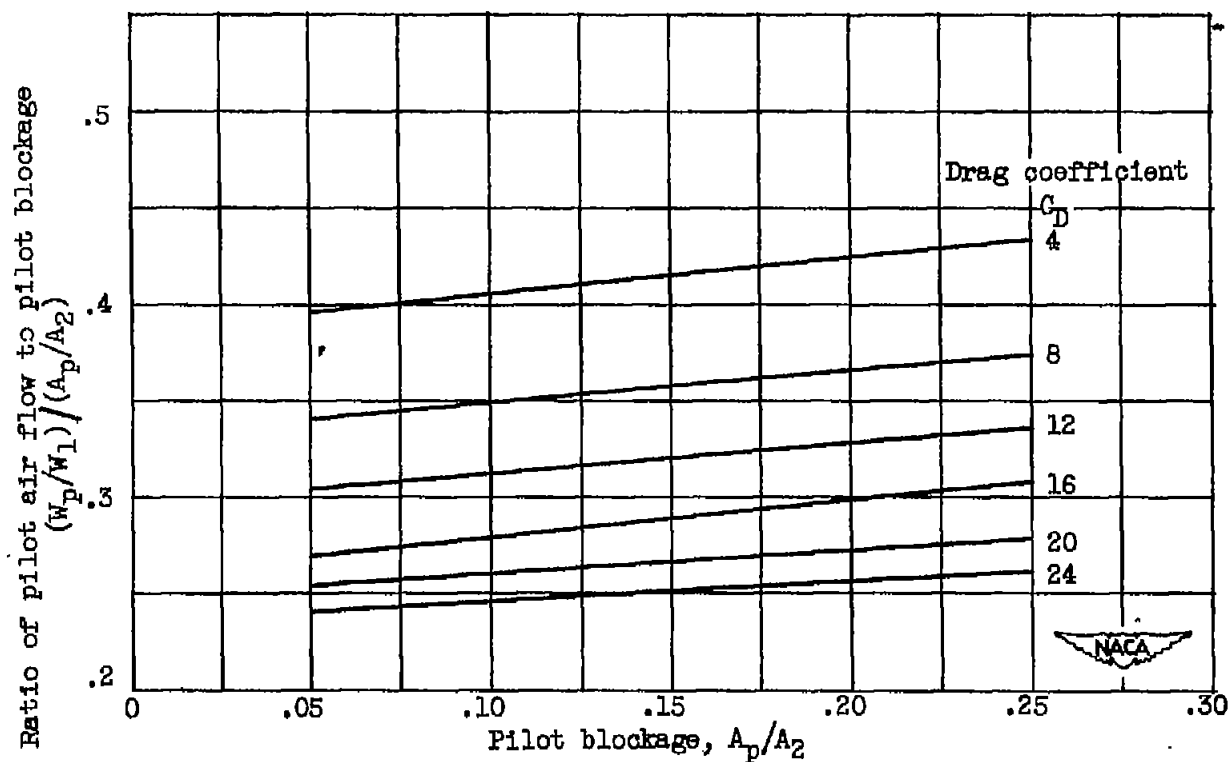


Figure 22. - Cross plot of curve intersection points from figure 21, showing variation of ratio of pilot air flow to pilot blockage with pilot blockage for various values of drag coefficient.

SECURITY INFORMATION

[REDACTED]

NASA Technical Library



3 1176 01435 6407

[REDACTED]